Available online at www.sciencedirect.com
ScienceDirect
Journal of Colloid and Interface Science 313 (2007) 612–629
JOURNAL OF Colloid and Interface Science
www.elsevier.com/locate/jcis

Emulsification in turbulent flow 2. Breakage rate constants

Nina Vankova [a], Slavka Tcholakova [a], Nikolai D. Denkov [a,*], Vassil D. Vulchev [b], Thomas Danner [c]

[a] *Laboratory of Chemical Physics & Engineering, Faculty of Chemistry, Sofia University, 1 James Bourchier Ave., 1164 Sofia, Bulgaria*
[b] *Faculty of Physics, Sofia University, 1164 Sofia, Bulgaria*
[c] *BASF Aktiengesellschaft GCT/P, L549, Ludwigshafen, Germany*

Received 20 October 2006; accepted 29 April 2007

Available online 3 May 2007

Abstract

Systematic experimental study of the effects of several factors on the breakage rate constant, k_{BR}, during emulsification in turbulent flow is performed. These factors are the drop size, interfacial tension, viscosity of the oil phase, and rate of energy dissipation in the flow. As starting oil–water premixes we use emulsions containing monodisperse oil drops, which have been generated by the method of membrane emulsification. By passing these premixes through a narrow-gap homogenizer, working in turbulent regime of emulsification, we study the evolution of the number concentration of the drops with given diameter, as a function of the emulsification time. The experimental data are analyzed by a kinetic scheme, which takes into account the generation of drops of a given size (as a result of breakage of larger drops) and their disappearance (as a result of their own breakage process). The experimental results for k_{BR} are compared with theoretical expressions from the literature and their modifications. The results for all systems could be described reasonably well by an explicit expression, which is a product of: (a) the frequency of collisions between drops and turbulent eddies of similar size, and (b) the efficiency of drop breakage, which depends on the energy required for drop deformation. The drop deformation energy contains two contributions, originating from the drop surface extension and from the viscous dissipation inside the breaking drop. In the related subsequent paper, the size distribution of the daughter drops formed in the process of drop breakage is analyzed for the same experimental systems.

Keywords: Kinetics of drop breakage; Emulsification in turbulent flow

1. Introduction

At sufficiently high surfactant concentrations, the outcome of the emulsification process is determined by the drop breakage only [1–14]. The classical studies of emulsification in turbulent flow by Kolmogorov [1] and Hinze [2] showed that the maximum diameter of stable drops, d_{MAX}, formed while emulsifying liquids of low viscosity, is determined by the balance between the fluctuations in the hydrodynamic pressure of the continuous phase and the drop capillary pressure, which opposes the drop deformation. A simple theoretical expression was derived [1,2] relating d_{MAX} with the rate of energy dissipation per unit mass of the fluid, ε (the main characteristic of the turbulent flow in the Kolmogorov's theory) and the interfacial tension of the drops, σ.

The theory for the maximum diameter of the stable drops was further developed for viscous and non-Newtonian drops [9–14]. Following the approach from Refs. [1,2], Davies [9] and Lagisetty et al. [10] used a stress balance to derive expressions for d_{MAX}. Davies [9] included the contribution from the viscous dissipation inside the drops, whereas Lagisetty et al. [10] considered the effects of the time required for drop deformation and of possible non-Newtonian rheological behavior of the drop phase. Calabrese et al. [11–14] suggested another approach, in which the energy required for drop deformation was compared to the kinetic energy of the turbulent eddies. Experiments for clarifying the effects of drop viscosity and interfacial tension on d_{MAX} were performed in Refs. [11–14], and a good agreement with the theoretical expressions was observed.

* Corresponding author. Fax: +359 2 962 5643.
E-mail address: nd@lcpe.uni-sofia.bg (N.D. Denkov).

0021-9797/$ – see front matter
doi:10.1016/j.jcis.2007.04.064

The maximum diameter of the stable drops is determined experimentally after a sufficiently long period of emulsification, when a steady-state drop-size distribution is reached. Along with this steady-state distribution, the rate of drop breakage is another important characteristic of the emulsification process, which is of great interest from practical and scientific viewpoints. For practice, the problem is important, because a very long emulsification time (or large number of passes of the emulsion through the homogenizer) might be needed to reach the steady state, e.g., for viscous oils and/or high interfacial tensions. From scientific viewpoint, the problem is challenging, because the kinetic aspects of the interactions between the turbulent eddies and the breaking drops are still poorly understood, and no general theoretical description of the kinetics of drop breakage is available.

Three main types of theoretical models for the rate of drop breakage in turbulent flow are discussed in literature (see the review in Ref. [15]). In the first type of models, the rate constant of drop breakage, k_{BR}, is constructed as a product of the reciprocal time of drop deformation (assumed to be equivalent to the characteristic frequency of drop deformation) and the efficiency of drop breakage [16,17]. In the second type of models, k_{BR} is considered as a product of the eddy–drop collision frequency and the efficiency of drop breakage [18–20]. In both cases, the efficiency of drop breakage is expressed as an exponential term, including the ratio of the surface energy for drop deformation and the kinetic energy of the turbulent eddies. In the third type of models (called "kinematic models"), k_{BR} is assumed equal to the inverse drop breakage time, which in turn is determined from the balance of stresses acting on the breaking drop [15,21–24]. Further explanations about these models are given in Section 6 below.

The above models of drop breakage are often implemented in the so-called "population balance equation" (PBE) to describe the temporal evolution of the drop-size distribution, which can be determined experimentally [16,18–20,25–30]. In several of the studies, the PBE was tested with emulsification experiments in the absence of surfactants, so that both drop breakage and drop–drop coalescence were simultaneously present [16,18–20]. The process of drop coalescence is still poorly understood, and as a consequence, the PBE in these studies included expressions for the rate of drop–drop coalescence, which were uncertain and also required verification [16,18–20]. Therefore, it turned out impossible to perform a direct, unambiguous verification of the drop breakage models in Refs. [16, 18–20], due to the strong coupling between the processes of drop breakage and drop coalescence.

In other studies, the drop breakage probability was determined by direct observation of drop breakage events in turbulent flow by a high-speed camera [31,32]. The probability for drop breakage was determined as a function of the drop diameter, d, at different Weber numbers, defined as $\mathrm{We} = Pd/\sigma$, where P is the applied pressure and σ is the interfacial tension. This approach has the advantage that the number of daughter drops, formed upon drop breakage, is directly determined in the observation. However, the method is time-consuming, so that only limited amount of data about the effects of the various factors of interest was obtained [31,32].

In Refs. [33,34], an effective breakage rate constant was determined from the observed decrease of the mean drop size with the emulsification time in stirred tanks. The experimental results were described by an empirical equation, which included several adjustable constants. The comparison of these results with the theoretical models is not straightforward, because the rate of decrease of the mean drop size is related in a complex way with the breakage rate constants of the drops with various sizes in the emulsion (see Section 4.5 in Ref. [35]).

In more elaborated studies by Narsimhan et al. [36–39], the change of drop-size distribution during emulsification in stirred tanks was used to determine k_{BR}. The experiments were performed in the absence of surfactants and, to minimize the possible effect of drop–drop coalescence, the oil was dispersed at very low volume fractions. To interpret the experimental data, the so-called "self-similarity" assumption was proposed, which relates the probability for formation of daughter drops of given size with the dependence of k_{BR} on drop size (see Refs. [36–39] for detailed explanations). The experimentally determined breakage rate constant was found to increase with the drop diameter, and to decrease with the interfacial tension and oil viscosity. Semi-empirical expression was proposed to describe these dependences [38].

In our previous studies [40–43] we explored experimentally and theoretically the effects of several factors (interfacial tension, oil viscosity, and rate of energy dissipation in the turbulent flow) on the maximum diameter of the stable drops, d_{MAX}, in emulsions prepared by narrow-gap homogenizer. We found that d_{MAX} in the inertial regime of emulsification is well represented by an equation proposed by Davies [9], and that the viscous oils are better emulsified in the viscous regime of turbulent emulsification.

The current paper is a direct continuation of our previous study [43], aimed to elucidate further the effects of several factors on the rate of drop breakage in turbulent flow. The emulsification of oils of different viscosities, ranging from 3 to 500 mPa s, is studied. Two surfactants are used, Na caseinate and Brij 58, to clarify the effect of interfacial tension. The experiments were performed at relatively high surfactant concentration and low oil volume fraction to avoid drop–drop coalescence. Different driving pressures were applied to quantify the effect of the rate of energy dissipation. As starting oil–water premixes we used emulsions containing monodisperse oil drops, which had been generated by the method of membrane emulsification. By passing these premixes through a narrow-gap homogenizer, we determined the evolution of the drop-size distribution, as a function of the emulsification time. The experimental data were analyzed by using a detailed kinetic scheme, which allowed us to evaluate k_{BR}, as a function of drop diameter and of the other factors studied. The results for k_{BR} are compared to theoretical models from literature and their modifications. The current paper is directly linked to the subsequent paper of this series [35], where the size distribution of the daughter drops, formed after breakage of a larger drop, is analyzed and discussed for the same emulsions.

2. Materials and methods

2.1. Materials

As emulsifiers we used the non-ionic surfactant polyoxyethylene-20 hexadecyl ether (Brij 58, product of Sigma) and the protein derivative sodium caseinate (Na caseinate; ingredient name Alanate 180; product of NXMP). The emulsifiers were used as received, with concentration of 1 wt% Brij 58 or 0.5 wt% Na caseinate in the aqueous phase. All solutions were prepared with deionized water, which was purified by a Milli–Q Organex system (Millipore), and contained 150 mM NaCl (Merck, analytical grade). The protein solutions contained also 0.01 wt% of the antibacterial agent NaN_3 (Riedel-de Haën, Seelze, Germany).

As dispersed phase we used the following oils: hexadecane with viscosity $\eta_D = 3.0$ mPa s (product of Merck), soybean oil with $\eta_D = 50$ mPa s (SBO, commercial product), and four silicone oils with $\eta_D = 50$, 95, 194, and 494 mPa s (denoted for clarity as SilXX, where XX denotes the oil viscosity in mPa s). Hexadecane and soybean oil were purified from surface-active contaminants by passing the oils through a glass column, filled with Florisil adsorbent [44]. The silicone oils were products of different companies (BASF, Rhodia and TDCS) and were used as received.

2.2. Emulsification procedures

All emulsions were prepared by a two-step protocol, which included two experimental techniques: (1) membrane emulsification, used to prepare the initial oil–water premix, and (2) emulsification with a narrow-gap homogenizer, which was used to quantify the kinetics of drop breakage in turbulent flow.

2.2.1. Membrane emulsification

An initial emulsion (oil–water premix) containing monodisperse oil drops, was first prepared by membrane emulsification. This method is based on the use of microporous membranes, made of glass, ceramics, or metal, and having relatively narrow pore-size distribution [45,46]. The dispersed phase (hexadecane, SBO, or silicone oil in our experiments) is emulsified by passing it through the membrane pores under pressure, into the continuous phase (the surfactant solution). We used a laboratory Microkit membrane emulsification module from Shirasu Porous Glass Technology (SPG, Miyazaki, Japan) [47–49], which works with tubular glass membranes of outer diameter 10 mm and working area of approximately 3 cm^2. Four membranes, with mean pore size of 1.1 μm (denoted as SPG1.1 in the text); 3.2 μm (SPG3.2); 10.7 μm (SPG10.7) and 19.3 μm (SPG19.3), were used for preparing initial emulsions with different drop diameters. After completion of this stage, samples for determination of the initial drop-size distribution (before starting the actual emulsification experiments in turbulent flow) were taken with a pipette.

The main advantage of using membrane emulsification for preparing the initial oil–water premix is that this method produces relatively monodisperse emulsions with sharp upper boundary in the drop-size distribution. Such emulsions ensure much better statistics for the change in the concentrations of the large drops in the emulsions, with the emulsification time, which was very helpful in determining the kinetic constants of drop breakup.

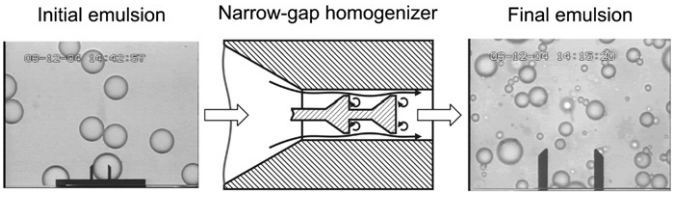

Fig. 1. Optical microscopy images of an initial emulsion prepared by membrane emulsification and of the final emulsion, obtained after 100 passes ($u = 100$) through the narrow-gap homogenizer. The distance between the vertical marks in the two photos is 20 μm.

2.2.2. Narrow-gap homogenizer

The second homogenization step was accomplished by 100 passes of the emulsion through a custom-made "narrow-gap" homogenizer with an axially symmetric cylindrical mixing head [42]. The mixing head contained a processing element, with two consecutive annular slits (each of them with gap-width of 395 μm and length of 1 mm), through which the oil–water mixture was passed under pressure, see Fig. 1. The drop breakage occurs predominantly in the intensive turbulent flow realized in the second narrow slit and in the zone just behind this slit, where the rate of energy dissipation is the highest [42].

The driving pressure for this emulsification step was provided by a gas N_2-bottle. Pressure control system was used to regulate the pressure during emulsification with an accuracy of ±500 Pa. Two driving pressures were used in the various series of experiments, $\approx 0.95 \times 10^5$ and $\approx 2.0 \times 10^5$ Pa, to clarify the effect of the rate of energy dissipation on the drop breakage rate constant. After each pass through the homogenizer, the emulsion was collected in a container attached to the outlet of the equipment (see Fig. 2 in Ref. [43]). Then the gas pressure in the inlet container was released, and the emulsion was poured back in the inlet container (under the action of gravity), by using a bypass tube. Afterwards, the gas pressure in the inlet container was increased again and the emulsion was pushed to make another pass through the homogenizer. In Table 1 we summarize the operating conditions for all systems discussed below.

After each of the first 10 passes, and then after each fifth pass, emulsion samples were taken for determination of the drop-size distribution. Thus we determined how the drop-size distribution and the mean drop size evolved, as functions of the number of passes (viz. of the emulsification time).

2.3. Determination of drop-size distribution, oil viscosity and interfacial tension

The drop-size distribution was determined by optical microscopy. The oil drops were observed and video-recorded in transmitted light by means of microscope Axioplan (Zeiss, Germany), equipped with objective Epiplan, ×50, and connected

Table 1
Operating conditions during emulsification of the systems studied. The processing element has two consecutive slits with gap-width of 395 μm and length 1 mm. The residence time and the rate of energy dissipation are calculated by the relations $\theta = V_{DIS}/Q$ and $\varepsilon = PQ/V_{DIS}$, respectively, where P is the applied pressure, Q is the flow rate, and V_{DIS} is the dissipation volume determined from Eq. (16) in Ref. [43]. Aqueous solutions of Brij 58 and Na caseinate were used as continuous phase with $\rho_C = 1.0$ g/cm^3. The other quantities are the mean volume-surface diameter of the initial oil–water premix, prepared by membrane emulsification, d_{32}^{INI}; oil volume fraction, Φ; viscosity of the oil phase, η_D; interfacial tension, σ; characteristic Kolmogorov size, d_{KI}, calculated by Eq. (16); Davies diameter, d_D, calculated by Eq. (15); diameter of the largest drops that could not break, d_K (see Section 4); and drop diameter, d_{RE}, corresponding to $Re_{DR} = 1$ (Eq. (22)) and average number of daughter drops formed after breaking of a mother drop with diameter d_{K+1} or $d_M = 50.8$ μm, calculated by Eq. (24) in Ref. [35]

Notation	Aqueous phase	Oil phase	Φ (%)	η_D (mPa s)	σ (mN/m)	Hydrodynamic conditions					Diameters						Average number of formed daughter drops, ν	
						$P \times 10^5$ (Pa)	$Q \times 10^{-3}$ (m^3/s)	$V_{DIS} \times 10^{-7}$ (m^3)	θ (ms)	$\varepsilon \times 10^5$ (J/(kg s))	d_{32}^{INI} (μm)	d_{KI} (μm)	d_D (μm)	d_K (μm)	d_{RE} (μm)	$\nu(d_{K+1})$	$\nu(d_M = 50.8)$ (μm)
C16_Br_P1	1 wt% Brij 58	C16	0.95	3	7.0 ± 0.1	0.93	0.095	1.33	1.40	0.67	33.0	9.5	8.9	5.0	5.5	10	18
SBO_Br_P1	150 mM NaCl	SBO	1.0	50	7.4 ± 0.1	0.914	0.086	1.37	1.60	0.57	32.6	10.5	19.0	16.0	40.9	41	97
SBO_Br_P2		SBO	1.0	50	7.4 ± 0.1	2.05	0.150	1.04	0.69	2.95	34.0	5.4	11.7	8	27.2	37	75
Sil50_Br_P1		Sil	0.6	50	10.8 ± 0.1	0.93	0.092	1.34	1.46	0.64	35.2	12.5	20.0	16	38.4	34	42
Sil100_Br_P1		Sil	0.3	95	10.3 ± 0.1	0.94	0.096	1.32	1.38	0.68	34.4	11.9	27.0	20.2	61.4	135	203
Sil200_Br_P2		Sil	1.0	194	10.5 ± 0.1	2.03	0.137	1.11	0.81	2.51	60.2	7.5	29.9	25.4	75.4	107	186
Sil500_Br_P2		Sil	1.0	494	11.7 ± 0.1	2.04	0.140	1.09	0.78	2.61	59.0	7.4	56.9	40.3	147	319	319
SBO_Br_P2_S		SBO	0.24	50	7.4 ± 0.1	2.05	0.16	0.98	0.62	3.32	11.1	5.2	11.3	8	26.4	13	–
C16_NaC_P1	Na caseinate	C16	1.4	3	28.8 ± 0.1	0.99	0.104	1.28	1.23	0.81	34.4	20.5	18.3	12.7	5.2	9	10
C16_NaC_P2	150 mM NaCl	C16	0.4	3	28.8 ± 0.1	2.13	0.159	0.99	0.63	3.40	33.7	11.6	10.4	8	3.6	11	13
SBO_NaC_P2		SBO	1.0	50	20.5 ± 0.1	2.03	0.150	1.04	0.69	2.93	44.2	10.0	14.7	16	27.2	59	86

to a CCD camera and video-recorder. The diameters of the oil drops were measured one by one, from the recorded video-frames, by using custom-made image analysis software operating with Targa$^+$ graphic board (Truevision, USA).

The viscosity of hexadecane and soybean oil was measured by capillary viscometer, whereas the viscosity of the silicone oils was measured on Gemini research rheometer (Bohlin & Malvern Instruments, UK) at the temperature of the emulsification experiments.

The equilibrium and the dynamic oil–water interfacial tensions were measured by a drop-shape-analysis of pendant oil drops and by the stopped jet method, respectively, as explained in Section 3.5 of Ref. [43].

3. Kinetic scheme for the process of drop breakage

In this section we present the kinetic model used for interpretation of the experimental data and for determination of the breakage rate constants, k_{BR}.

3.1. Main assumptions of the model

The main assumptions of the model are: (1) The drop–drop coalescence is negligible; (2) The process of drop breakage is considered as an irreversible reaction of first order; (3) The drops are classified in discrete drop–diameter intervals—all drops falling in a given interval are considered as having the same diameter, d_S, which is the average diameter of the interval; (4) The intervals are chosen in such a way, that the ratio of the average drop volumes for two consecutive intervals is equal to two, i.e. $v_{S+1} = 2v_S$. This procedure defines a geometric grid for discretization of the drop sizes and was originally suggested by Bleck [50]. The used discretization scheme falls in the category of the so-called "fixed pivot techniques," see Section 3 in Ref. [51]. Note, however, that the geometric grid used here is different from the discretization grid used in Ref. [51]. (5) Kinetic equations are constructed for the number concentration of the drops falling in a given interval, $n_S = n(d_S)$, under the assumption that the drop breakage occurs only in the processing element of the homogenizer, which is modeled as a reactor with ideal displacement of the fluid [52].

More detailed description of the system and the equations stemming from the above assumptions are presented in the following Sections 3.2–3.5.

3.2. Discrete description of the drop-size distribution

We consider a hypothetical emulsion, which contains drops with discrete set of volumes (diameters). The volume of the smallest drops in the system is denoted as v_0 and the respective drop diameter is d_0. The volumes of the larger drops are $2v_0$, $4v_0$, $8v_0$, etc. The volume of the largest drops in the emulsion under consideration is $2^N v_0$, where N is an integer, which depends on the specific emulsion. The drop diameters in this emulsion are d_0, $\sqrt[3]{2}d_0$, $\sqrt[3]{2^2}d_0, \ldots, \sqrt[3]{2^N}d_0$. To simplify the notation, we denote these diameters by $d_0, d_1, d_2, \ldots, d_N$, where $d_S = \sqrt[3]{2^S}d_0$ and S is an integer between 0 and N. The

diameter of the smallest drops, $d_0 = 0.25$ μm, was chosen to be close to the resolution of the optical microscope used to determine the experimental drop-size distribution (direct checks showed that the final results and conclusions do not depend on the particular choice of d_0, if it is chosen to be <0.5 μm).

The width of the interval with average diameter d_S is denoted by Δy_S and was chosen to be proportional to d_S [53]. In other words, the ratio of the widths of two neighboring intervals, $\Delta y_{S+1}/\Delta y_S$, is equal to the ratio of the neighboring diameters, $d_{S+1}/d_S = 2^{1/3}$, which leads to the following definition for the boundaries of the interval around d_S:

$$0.885 d_S < d_S < 1.115 d_S. \tag{1}$$

In the studied emulsions, we distinguish three qualitatively different types of drops: (1) The largest drops with diameter d_N could only disappear due to their breakage and cannot be formed from other (larger) drops, because no such larger drops are present. (2) The drops with diameter smaller than d_N and larger than a certain diameter, d_K, can break and, simultaneously, can be formed as a product of breaking of larger drops. (3) The drops with diameter $d_S \leqslant d_K$ could only be formed as a product of breakage of larger drops. The diameter of the largest drops that could not break, d_K, is found as a part of the overall solution of the problem (see Section 4 below). In our discrete drop-size distribution, d_K is the analogue of the maximum diameter of the stable drops in the Kolmogorov–Hinze theory of emulsification [1,2].

3.3. Determination of drop number concentration, n_S, from the experimental data

To determine the breakage rate constants, k_{BR}, from the experimental data, we analyze the changes in the number concentration, n_S, of drops with given diameter d_S, after passing the emulsion through the homogenizer in multiple passes. To find the experimental dependence of n_S on the number of passes, u, we classified the drop diameters measured in the emulsion after a given pass, into discrete intervals as explained in Section 3.2. To determine the number concentration, n_S, from the number of drops, N_S, measured to be in the interval with mean diameter d_S, we used the following identities:

$$n_S = n(d_S) \equiv \frac{N_S}{V_{\mathrm{EM}}} = \frac{N_S \Phi}{V_{\mathrm{OIL}}} = \frac{6\Phi}{\pi} \frac{N_S}{\sum_{i=0}^{N} N_i d_i^3}, \tag{2}$$

where Φ is the oil volume fraction, V_{EM} is the total emulsion volume, V_{OIL} is the total volume of emulsified oil, and N_i is the number of drops, which are measured microscopically to have diameter d_i.

3.4. Distribution by size of the daughter drops formed upon drop breakage

To design kinetic equations for the evolution of the drop-size distribution during emulsification, we should consider the probability for formation of a "daughter" drop of diameter d_S as a result of breakage of larger "mother" drop with diameter d_M $(K < M \leqslant N)$. The analysis of our experimental results shows clearly [35] that the breakage of a drop with diameter d_M leads to formation of several daughter drops, which might have diameters in the range between d_0 and d_{M-1}. The fraction of the volume of the mother drop, which is transformed into drops with diameter d_S $(0 \leqslant S \leqslant M-1)$ is denoted by $p_{S,M}$. Taking into account the fact that in our model, by definition $v_M/v_S = 2^{M-S}$, one can deduce that the value $(2^{M-S} p_{S,M})$ gives the average number of drops with diameter d_S, which are formed as a result of breakage of one mother drop with diameter d_M. The mass balance requires that the total volume of the daughter drops should be equal to v_M, which corresponds to the relation:

$$\sum_{S=0}^{M-1} p_{S,M} = 1, \quad K < M \leqslant N. \tag{3}$$

Equation (3) should be satisfied for every value of M in the interval $K < M \leqslant N$, where K is the index of the largest non-breaking drops and N is the index of the largest drops in the emulsion.

3.5. Kinetic equations describing the drop-size evolution during emulsification

To formulate the kinetic equations, we assume that the drop breakage occurs only inside the processing element of the homogenizer, which is considered as a "reactor" with ideal displacement [52], see Fig. 2. The ideal displacement model implies that there is no longitudinal mixing of the fluid elements, as they move along the reactor, and that all fluid elements travel for the same period of time (so-called "residence time," θ) from the inlet to the outlet of the reactor [52]. Since the composition of the emulsion entering the reactor during a given pass with number u $(1 \leqslant u \leqslant 100)$ does not depend on time, a steady-state drop-size distribution is established *inside the reactor* within a very short period after starting this pass. One can expect that the establishment of the steady-state requires a period, comparable to the residence time of the emulsion inside the homogenizer head (≈1 ms), which is much shorter than the overall duration of the emulsion pass through the homogenizer (≈15 s)—therefore, the drop-size distribution obtained after a given pass is determined exclusively by the steady-state period of emulsification in the reactor. For simplicity and without making a significant error, we assume in the following consideration that the steady-state is reached immediately after starting the flow in the element.

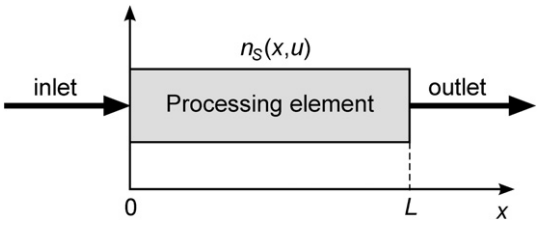

Fig. 2. Schematic presentation of the processing element as a plug–flow reactor with ideal displacement. The number concentration of drops with mean diameter d_S, $n_S(x,u)$, depends on the distance from the inlet of the processing element, x, and on the number of the emulsion pass through the homogenizer, u.

During the steady-state period, the number concentration of drops with diameter d_S, which is denoted by $n_S(x,u)$, depends only on the distance, x, from the beginning of the reaction zone [52], see Fig. 2. Thus, we can formulate the following differential equation, describing the decrease of the concentration of the largest drops with diameter d_N along the processing element (valid for any pass with number u):

$$U_1\frac{\mathrm{d}n_N(x)}{\mathrm{d}x} = -k_N n_N(x), \tag{4}$$

where U_1 is the average linear velocity of the fluid along the processing element, x is the distance from the beginning of the element, $n_N(x)$ is the number concentration of the largest drops in the emulsion, and k_N is the breakage rate constant for these drops.

The differential equation, which describes the number concentration, n_S, of drops with diameter d_S, which could simultaneously break and form during emulsification, is:

$$U_1\frac{\mathrm{d}n_S(x)}{\mathrm{d}x} = -k_S n_S(x) + \sum_{M=S+1}^{N} 2^{M-S} p_{S,M} k_M n_M(x), \quad \text{for } K < S < N, \tag{5}$$

where the first term in the right-hand side of Eq. (5) gives the rate of drop breakage, whereas the second term describes the rate of formation of these drops, as a result of breakage of larger drops. The multiplier $(2^{M-S} p_{S,M})$ gives the average number of drops with diameter d_S, which are formed from the breakage of one drop with diameter d_M, where $N \geqslant M > S$.

The drops with diameter $d_S \leqslant d_K$ could be formed only as a result of breakage of larger drops, which means that the first term in Eq. (5) is zero and the kinetic equation simplifies to:

$$U_1\frac{\mathrm{d}n_S(x)}{\mathrm{d}x} = \sum_{M=K+1}^{N} 2^{M-S} p_{S,M} k_M n_M(x), \quad \text{for } 0 \leqslant S \leqslant K. \tag{6}$$

The solution of the set of Eqs. (4)–(6) can be found explicitly for each pass, u. For the first pass of the emulsion through the reactor, $u = 1$, we can use as initial conditions:

$$n_S(u=1, x=0) = n_S^0, \quad \text{for } 0 \leqslant S \leqslant N, \tag{7}$$

where n_S^0 is the number concentration of the drops with diameter d_S in the initial emulsion (the premix), which was prepared by membrane emulsification. The general solution for the concentrations of the drops of various sizes along the reactor, $n_S(x)$, during the first pass of the emulsion through the reactor $(u = 1)$ can be written as follows:

$$n_N(x) = n_N^0 \exp\left(-\frac{k_N x}{U_1}\right), \tag{8}$$

$$n_S(x) = \exp\left(-\frac{k_S x}{U_1}\right)\left(\text{const} + \frac{1}{U_1}\sum_{M=S+1}^{N} 2^{M-S} p_{S,M} k_M \int \exp\left(\frac{k_S x}{U_1}\right) n_M(x)\,\mathrm{d}x\right), \quad \text{for } K < S \leqslant N-1, \tag{9}$$

$$n_S(x) = n_S^0 + \frac{1}{U_1}\sum_{M=K+1}^{N} 2^{M-S} p_{S,M} k_M \int_0^x n_M(\xi)\,\mathrm{d}\xi, \quad \text{for } 0 \leqslant S \leqslant K, \tag{10}$$

where the constant in Eq. (9) is found from the initial condition at $x = 0$. The integrals in Eqs. (9) and (10) were evaluated analytically (resulting in explicit but long expressions), after the expressions for the concentrations of the larger drops $n_M(x)$ were obtained by solving the respective equations for these drops $(M > S)$. Thus by solving one after the other Eqs. (8)–(10), starting with the largest drops in the emulsion, $S = N$, we obtain a chain of explicit expressions for $n_S(x)$ for all values of S between 0 and N.

Experimentally, we measure the drop number concentration at the outlet of the homogenizer, i.e., at $x = L$, see Fig. 2. After substituting $x = L$ in Eqs. (8)–(10) and taking into account that $(L/U_1) = \theta$ is the residence time of the drops in the processing element, we obtain explicit expressions for the concentrations of the drops with different sizes at the outlet of the equipment after the first pass through the homogenizer. The result for the largest drops in the emulsion reads:

$$n_N(u=1, x=L) = n_N^0 \exp\left(-\frac{k_N L}{U_1}\right) = n_N^0 \exp(-k_N\theta). \tag{11}$$

The solution for the number concentration of the second fraction of drops, n_{N-1}, having a diameter d_{N-1}, is:

$$n_{N-1}(u=1, x=L) = \left(n_{N-1}^0 - \frac{2p_{N-1,N}k_N n_N^0}{k_{N-1}-k_N}\right)\exp(-k_{N-1}\theta) + \frac{2p_{N-1,N}k_N n_N^0}{k_{N-1}-k_N}\exp(-k_N\theta), \tag{12}$$

where k_{N-1} and k_N are the breakage rate constants for drops with diameters d_{N-1} and d_N, respectively; n_{N-1}^0 and n_N^0 are their concentrations in the initial premix; and $2p_{N-1,N}$ gives the average number of drops with diameter d_{N-1}, which are formed as a result of breakage of a single drop with diameter d_N. It is seen from Eq. (12) that the concentration of drops with diameter d_{N-1} at the outlet of the processing element depends not only of the rate constant of breakage of these drops, k_{N-1}, but also on the rate of their formation from the largest drops, viz. on the values of k_N and $p_{N-1,N}$. In a similar way, we derived expressions for the number concentrations of the smaller drops in the emulsion with diameters, $d_{N-2}, d_{N-3}, \ldots, d_0$.

To describe the evolution of the number concentration of the various drops, after different number of passes through the homogenizer, $n_S(u > 1)$, we solved Eqs. (4)–(7) by using as initial conditions for the pass of number u the number concentrations, which were calculated for the previous pass, $n_S(u-1)$. For example, for the second pass through the homogenizer we solve Eq. (4) for the largest drops, by using Eq. (11) instead of Eq. (7) as an initial condition. The result for arbitrary $u \geqslant 1$ reads:

$$n_N(u, x=L) = n_N^0 \exp(-uk_N\theta) = n_N^0 \exp(-k_N t_{\mathrm{EM}}), \quad u \geqslant 1, \tag{13}$$

where u is the number of passes of the emulsion through the homogenizer and n_N^0 is again the number concentration of the drops in the initial premix obtained by membrane emulsification. Note that the product $t_{EM} = u\theta$ gives the total time of emulsion residence inside the processing element (in the reactor), that is, t_{EM} is the total actual emulsification time.

In a similar way, we were able to obtain explicit expressions for the number concentrations of all drops in the emulsion, as functions of the number of passes through the homogenizer, u. For example, the respective equation for the drops with diameter d_{N-1} is

$$n_{N-1}(u, x = L) = \left(n_{N-1}^0 - \frac{2p_{N-1,N}k_N n_N^0}{k_{N-1} - k_N}\right)\exp(-uk_{N-1}\theta) + \frac{2p_{N-1,N}k_N n_N^0}{k_{N-1} - k_N}\exp(-uk_N\theta), \quad u \geqslant 1. \tag{14}$$

The equations for the smaller drops are rather long and will not be reproduced here.

Therefore, Eqs. (13)–(14) and their counterparts for the smaller drops in the emulsions, combined with the initial drop-size distribution measured before starting the emulsification in turbulent flow, n_S^0, are used for interpretation of the experimental data, which are the drop-size distributions, determined after different number of passes of the emulsion through the narrow-gap homogenizer. By comparing the calculated with the measured drop-size distributions after different number of passes we were able: (i) to determine the rate constants of drop breakage, and (ii) to gain non-trivial information about the constants, $p_{S,M}$, i.e., for the size distribution of the daughter drops, obtained as a result of breakage of one larger drop.

The direct determination of all constants $p_{S,M}$ from the interpretation of the experimental data by the kinetic scheme outlined above is impossible, because the number of unknown constants is much larger than the number of equations. Indeed, the constructed set consists of $(N + 1)$ equations, describing the evolution of the number concentration of drops with diameters between d_0 and d_N, plus $(N - K)$ equations expressing the mass balance of the breaking drops, Eq. (3). On the other hand, we have $(N - K)$ unknown breakage rate constants for the drops larger than d_K, as well as $(N - K)(N + K + 1)/2$ unknown constants of type $p_{S,M}$. Since the number of unknown constants is much larger than the number of equations, we encounter an undetermined mathematical problem and should make additional assumptions for the constants $p_{S,M}$ to solve the set of equations [39].

The detailed procedure used for determination of the constants $p_{S,M}$ is described in our subsequent paper [35]. Here we outline only the main features of the model daughter drop-size distributions (expressed through the constants $p_{S,M}$), which we found to describe the experimental data for all emulsions studied. Briefly, based on the analysis of the drop-size distribution histograms, determined after subsequent passes of a given emulsion through the homogenizer, we propose the so-called "combined model" [35]. In this model we split the size-distribution of the formed daughter drops into two regions—small daughter drops with diameter $d_S \leqslant d_K$ and large daughter drops with diameter $d_S > d_K$, see Fig. 3. For reasons explained in Ref. [35], we assume that the number probability for formation of the small daughter drops ($d_S \leqslant d_K$) is proportional to the number concentration of the respective drops (with the same diameter d_S) in the final emulsion, obtained after 100 passes of the emulsion through the homogenizer, see Eq. (9) in Ref. [35]. The constant of proportionality, denoted by b_M, depends on the size of the breaking mother drop, d_M, and is determined from the mass balance, see Eq. (3) above and Eq. (14) in Ref. [35]. Next, we assume that the number probability for formation of the larger drops ($d_K < d_S < d_{M-1}$) is *equal* to the number probability for formation of the drops with size d_K (see Eqs. (12) and (13) in [35]), except for the largest daughter drops ($d_S = d_{M-1}$), for which the number probability was assumed to be *proportional* to that of d_K with a constant of proportionality, denoted by b_2 (Eq. (11) in [35]). The constant b_2 does not depend on the size of the breaking drop, d_M, and on the number of passes, u (though b_2 depends on the composition of the emulsion and the hydrodynamic conditions during emulsification). Therefore, the proposed combined model includes only one adjustable parameter for a given emulsion, b_2, related to the probabilities for the formation of the daughter drops, which was determined (along with the kinetic constants k_S) by comparing the theoretical predictions for the evolution of the number concentrations of the drops on the number of emulsion passes through the homogenizer, $n_S(u)$—see the following Section 4. In practice, b_2 was determined by the method of trials and errors—assuming a certain value, we first calculated all constants $p_{S,M}$ from Eqs. (9), (11)–(14) in Ref. [35] and then used the procedure from Section 4 to determine the values of k_S. If the value of b_2 was inappropriately chosen, we could not find a set of kinetic constants k_S that describes the entire set of data for $n_S(u)$. In contrast, when the appropriate value of b_2 was used, we could describe the experimental data $n_S(u)$ for all drops and after all passes of the emulsion through the homogenizer. Direct numerical checks showed that the appropriate value of b_2 was unique and that the obtained set of constants $p_{S,M}$ and k_S was stable—no qualitatively different multiple solutions could be obtained within the frames of the used model. Note that the used procedure reduced the number of unknown constants to $(N - K + 1)$ only, which is much smaller than the number of

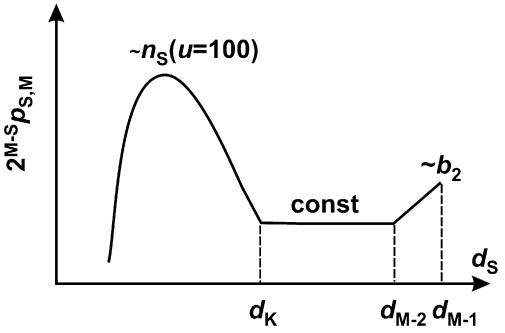

Fig. 3. Schematic presentation of the number probability for formation of daughter drops, as a function of the daughter drop diameter.

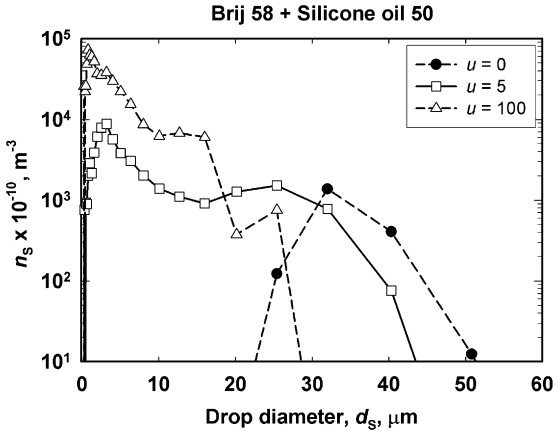

Fig. 4. Experimental data for the number concentration of the drops, as a function of drop diameter, in emulsion Sil50_Br_$P1$ (see Table 1): $u = 0$ (●) is for the premix, $u = 5$ (□) is after 5 passes, and $u = 100$ (△) is after 100 passes of the emulsion through the homogenizer.

equations $(2N - K + 1)$ and the number of experimental data sets to be fitted by these constants.

In the following sections of the current paper we discuss only the values of the breakage rate constants, k_{BR}, whereas the results for $p_{S,M}$ are described and discussed in the subsequent paper of the series, Ref. [35].

4. Determination of the breakage rate constants from the experimental data

Typical histograms for the initial monodisperse emulsion (the premix), and for the same emulsion after 5 and 100 passes through the homogenizer, are presented in Fig. 4. One sees from Fig. 4 that the number concentration of the largest drops decreases due to their breakage after the first pass, whereas the concentration of the smaller drops increases. From such histograms we can construct the dependence $n_S(u)$—see Fig. 5 below.

Equation (13) shows that the evolution of the number concentration of the largest drops, n_N, is independent of the breakage of the other drops in the emulsion. Therefore, we can determine k_N without information on how the smaller drops break. In contrast, to determine the breakage rate constant of the next fraction of drops, k_{N-1}, we need the value of $p_{N-1,N}$, which is not known in advance. The problem for determination of the rate constant for the smaller drops, k_{N-2}, is even more complex, because these drops could form in the process of breakage of the larger drops with diameters d_N and d_{N-1}. Thus, to describe the dependence of $n_{N-2}(u)$ we need the values of $k_N, k_{N-1}, k_{N-2}, p_{N-1,N}, p_{N-2,N}, p_{N-2,N-1}$. To illustrate the procedure for determination of k_{BR} from the experimental data, we demonstrate below the data analysis procedure under the assumption that the values of $p_{S,M}$ are known (i.e., they are calculated from Eqs. (9), (11)–(14) in Ref. [35], after assuming a certain value for the constant b_2).

From the best fit of the experimental data for $n_S(u)$ by equations similar to Eqs. (13) and (14) above, one can determine the values of k_S. Note that the values for the drops larger than d_S (viz. $k_{S+1}, k_{S+2}, \ldots, k_N$), which are determined from the best fits to the number concentrations of the respective drops (i.e., with diameters $d_{S+1}, d_{S+2}, \ldots, d_N$) are introduced into the kinetic equation for n_S, so that the only adjustable parameter in the equation for the drops with diameter d_S is k_S.

To illustrate this procedure, we present in Fig. 5 the experimental data, along with the best fits of the dependence $n_S(u)$ for the drops having diameters $d_K \leqslant d_S \leqslant d_N$ for one of the systems studied, Sil50_Br_p1 (see Table 1 for detailed description). For this particular emulsion, the indexes $K = 18$ and $N = 22$, which corresponds to $d_K = 16$ μm and $d_N = 40$ μm. One sees from Fig. 5 that the experimental data are well represented by the theoretical fits for all values of S varied between K and N. The concentration of the largest drops in the system decreases to zero after the first 8 passes, whereas the concentration of the drops with diameter d_{N-1} decreases more slowly, see Fig. 5a. These different rates of drop disappearance lead to different values of k_N and k_{N-1} (225 and 140 s^{-1}, respectively). The number concentrations of the drops with diameters d_{N-2} and d_{N-3} first increase (due to the formation of these drops after breakage of the larger drops) and than decrease, see Figs. 5b and 5c. The breakage rate constants for these drops were determined as 20 and 7 s^{-1}. The concentration of the drops with diameter $d_{N-4} = 16$ μm increases during all passes, see Fig. 5d. This means that the rate of their formation is significantly larger than the rate of their breakage during the entire emulsification procedure. For these drops we cannot determine k_{BR}, because the breakage rate is too slow to be significant in the timeframe of our experiments. We consider these drops as the largest drops, which could not break, with a diameter d_K. These drops remain in the final emulsion obtained after 100 passes through the homogenizer.

Let us compare now the values of d_K determined as explained above, with the diameter of the maximum stable drops in the final emulsions (after 100 passes). As shown in our previous paper [43], the maximum drop diameter (associated with the experimental data for d_{V95}) was described well by Davies' equation [9]:

$$d_{\mathrm{D}} = A_3\left(1 + A_4\frac{\eta_{\mathrm{D}}\varepsilon^{1/3}d_{\mathrm{D}}^{1/3}}{\sigma}\right)^{3/5}\sigma^{3/5}\rho_{\mathrm{C}}^{-3/5}\varepsilon^{-2/5} = A_3\left(1 + A_4\frac{\eta_{\mathrm{D}}\varepsilon^{1/3}d_{\mathrm{D}}^{1/3}}{\sigma}\right)^{3/5} d_{\mathrm{KI}}, \tag{15}$$

where σ is the interfacial tension, ρ_{C} is the mass density of the continuous phase, η_{D} is the drop oil viscosity, ε is the rate of energy dissipation per unit mass, and d_{KI} (having the dimension of length) is defined as:

$$d_{\mathrm{KI}} = \sigma^{3/5}\rho_{\mathrm{C}}^{-3/5}\varepsilon^{-2/5}. \tag{16}$$

In Ref. [43] we found that the best description of the experimental data for d_{V95} with Eq. (15) is obtained at $A_3 = 0.86$ and $A_4 = 0.37$.

One could expect that the value of d_K (diameter of the largest drops that cannot break in our kinetic scheme) should approximately correspond to the value of the maximum drop diameter, d_{D}, calculated by Eq. (15). The comparison of these two

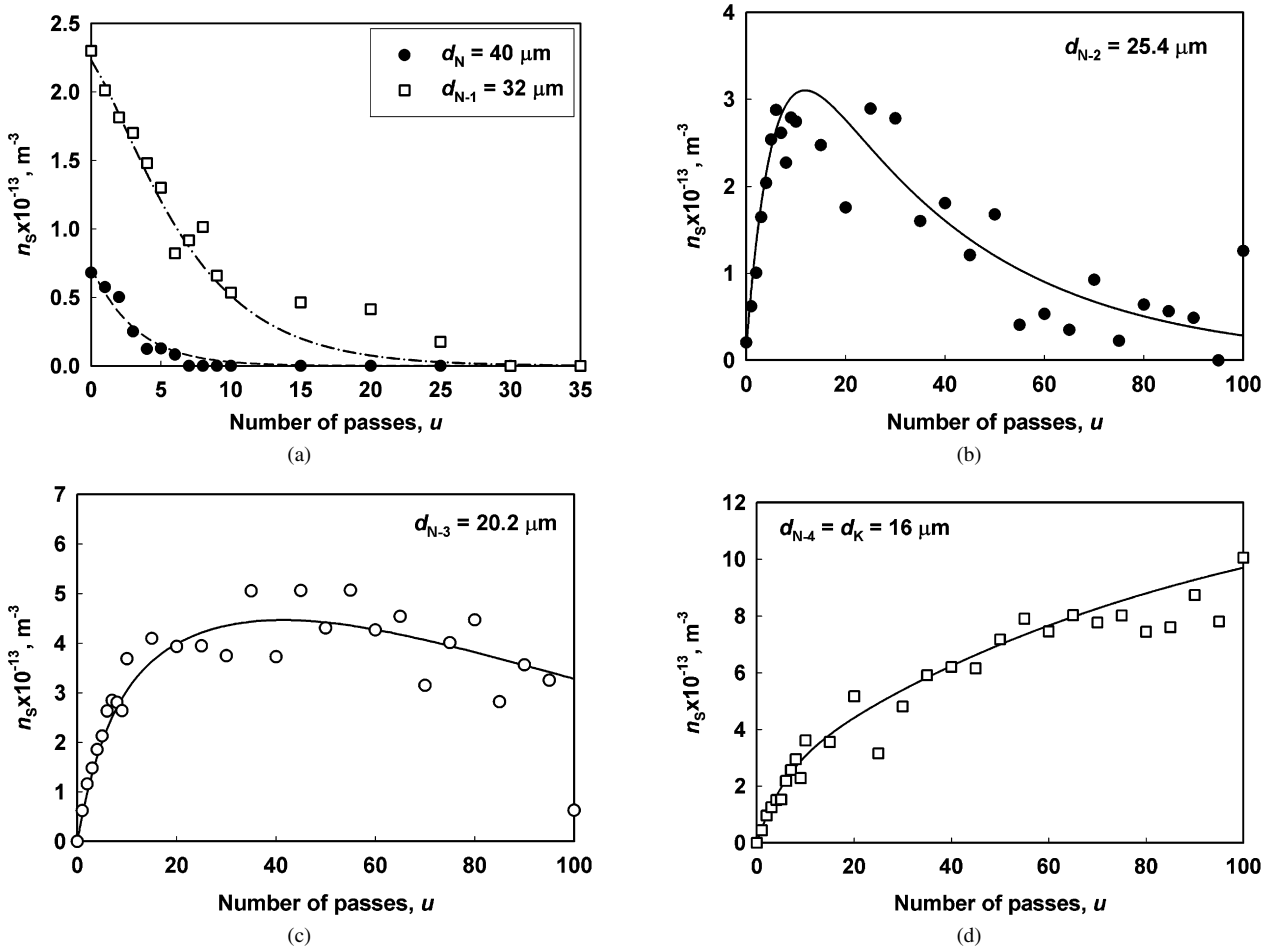

Fig. 5. Experimental data (●, □) for the number concentration, n_S, vs the number of passes of the emulsion through the homogenizer, u, along with the best fits, according to the kinetic scheme (- · · ·, - - -) in the system Sil50_Br_$P1$ for drops with diameters: (a) $d_N = 40$ μm (●) and $d_{N-1} = 32$ μm (□); (b) $d_{N-2} = 25.4$ μm; (c) $d_{N-3} = 20.2$ μm and (d) $d_{N-4} = d_K = 16$ μm.

characteristic diameters is presented in Table 1. One sees that the values of d_D are higher by 20–40% than the values of d_K. In fact, we found that d_D falls in the interval of drops with diameter d_{K+1}, which have relatively small, but still measurable breakage rate constant. We can conclude from this comparison, that the value of d_D is determined by the largest drops, which have survived the emulsification process for the specific characteristic time of our experiments, $t_{EXP} = 100 \times \theta$, but could break and would disappear, if much longer emulsification time was used. Because the breakage rate constant, $k(d_{K+1})$, is smaller than the inverse characteristic time of our experiment, $t_{EXP} = 100 \times \theta$, some noticeable fraction of drops with diameter $d_{K+1} \approx d_D$ have remained in the final emulsions after 100 passes, only because the emulsification time was not sufficiently long to allow breaking of these drops, see Fig. 5c.

In other words, the steady-state observed after 100 passes of the emulsion through the homogenizer is due to the rapid decrease of the breakage rate constant when the largest drops in the emulsion become with diameter $d \approx d_D$. If we have performed experiments with much longer characteristic time (e.g., with 1000 instead of 100 passes of the emulsion through the homogenizer), the maximum diameter of the stable drops in the final emulsions (and, respectively, the constant A_3 in Eq. (15)) would be slightly smaller. For a detailed theoretical investigation and discussion of this relation between the experimentally determined maximum drop diameter and the duration of the emulsification process see Refs. [28,29].

5. Experimental results for the breakage rate constant

In this section we present and discuss briefly the experimental results for the breakage rate constant, k_S, for the various emulsions. More detailed discussion of the effects of the various factors on k_S is presented in the following section.

As explained in the Section 4, the effect of drop size on k_{BR} is very strong (see also Figs. S1–S3 in the supporting material). The breakage rate constants decreased very rapidly with the decrease of drop size and became negligible at drop diameters $d < d_D$.

The effect of oil viscosity on the dependence $k_{BR}(d)$ was studied with silicone oils at two different rates of energy dissipation, $\varepsilon = 0.6 \times 10^5$ and $\varepsilon = 2.5 \times 10^5$ $J/(\mathrm{kg\,s})$ (see Fig. S1 and Table 1). At the lower value of ε we performed experiments with oils of viscosity $\eta_D = 50$ mPa s and $\eta_D \approx 100$ mPa s (Fig. S1A), whereas experiments with oils having viscosities of 200 and 500 mPa s were performed at the higher value of ε. All

emulsions were stabilized by 1 wt% Brij 58, which ensures interfacial tension of around 10.5 mN/m in all these systems. As seen from Fig. S1, the breakage rate constants decrease significantly with the increase of η_D for given drop size $d > d_K$, at fixed other conditions.

The effect of interfacial tension on k_{BR} was studied with hexadecane-in-water ($\eta_D = 3$ mPa s) and soybean oil-in-water ($\eta_D = 50$ mPa s) emulsions, stabilized by two different surfactants, 1 wt% Brij 58 and 0.5 wt% Na caseinate. The interfacial tensions for the hexadecane emulsions were 7.0 and 28.8 mN/m, whereas for the SBO emulsions they were 7.4 and 20.5 mN/m, respectively [43]. The emulsification experiments for the hexadecane emulsions were performed at $\varepsilon \approx 0.7 \times 10^5$ J/(kg s), whereas $\varepsilon \approx 2.9 \times 10^5$ J/(kg s) was applied for the SBO emulsions. The results presented in Fig. S2 show that the dependence of k_{BR} on the interfacial tension, σ, is strong—the values of k_{BR} for emulsions stabilized by Na caseinate, which have higher interfacial tension, are much lower than those for Brij-stabilized emulsions. Just for example, for the hexadecane emulsion prepared with Brij 58 ($\sigma = 7.0$ mN/m) k_{BR} was ≈ 400 s^{-1}, whereas k_{BR} for the emulsion stabilized by Na caseinate ($\sigma = 28.8$ mN/m) was ≈ 22 s^{-1} for drops with $d = 20$ μm, see Fig. S2A.

The effect of the rate of energy dissipation on k_{BR} is illustrated in Fig. S3. For hexadecane emulsions stabilized by Na caseinate, the increase of ε from 0.8 to 3.4×10^5 J/(kg s) leads to a 20-fold increase of k_{BR} at $d = 20$ μm. Similarly, for SBO emulsions stabilized by Brij 58 we observe that k_{BR} increases more than 10 times when ε increases from 0.57×10^5 to 2.95×10^5 J/(kg s) for drops with $d = 20$ μm; the respective increase of k_{BR} is more than 100 times for drops with $d = 16$ μm, see Fig. S3B.

In conclusion, all factors studied (drop diameter, oil drop viscosity, interfacial tension, and rate of energy dissipation) affect significantly k_{BR}. For all of the systems studied, k_{BR} becomes negligible (in the timeframe of our experiment), when d becomes smaller than the value of d_D, as calculated from Eq. (15).

6. Comparison of the experimental results for k_{BR} with theoretical models

As explained in the introduction, three main types of models are discussed in literature [15–24,54,55]: (1) In the first type, k_{BR} is presented as a product of the reciprocal time of drop deformation and the efficiency of drop breakage. (2) k_{BR} is presented as a product of the eddy–drop collision frequency and the efficiency of drop breakage. (3) k_{BR} is assumed equal to the inverse drop breakage time, which in turn is determined from the stress balance in the deforming drop [15,21–24]. In this section we briefly describe some of these models and their modifications, which are suggested in the current study for better description of our experimental data. The predictions of the various models are compared with the experimental data and, on this basis, these models are discussed.

6.1. Models based on drop deformation time and activation energy

The model for the rate of drop breakage proposed by Coulaloglou and Tavlaridies [16] is based on the assumption that k_{BR} is a product of the fraction of drops (from the total number of drops with given size in the emulsion), which have sufficiently high energy to undergo drop breaking, and the reciprocal time needed for the drop breakage to occur:

$$k_{BR} = \left(\frac{1}{\text{breakage time}}\right)\left(\begin{array}{c}\text{fraction of}\\ \text{drops breaking}\end{array}\right) \approx \frac{1}{t_{BR}} \exp\left(-\frac{E_\sigma}{E_{KIN}}\right). \quad (17)$$

The drop breakage time is estimated by assuming that it is approximately equal to the characteristic time for drop deformation, $t_{BR} \approx t_{DEF}$ (see Eqs. (23) and (25) below). The exponential factor is assumed equal to the ratio of the surface energy required for drop deformation and the mean kinetic energy of the turbulent eddies. The drop surface energy is estimated as [16]:

$$E_\sigma \sim \pi d^2 \sigma. \quad (18)$$

The mean turbulent kinetic energy, $E_{KIN}(d)$, of an eddy with size d, can be estimated from the theory of turbulence [16], by multiplying the mass and the mean square velocity, $\langle U^2 \rangle$, of the eddy:

$$E_{KIN} \sim \pi \rho_D d^3 \langle U^2 \rangle / 6, \quad (19)$$

where ρ_D is the mass density of the dispersed phase. For the inertial subrange, $\langle U^2 \rangle$ is given by [1,2,56]

$$\langle U^2 \rangle \sim \varepsilon^{2/3} d^{2/3}. \quad (20)$$

Following Refs. [16,29], we assume that the eddies with size comparable to the drop diameter, d, are most efficient in causing drop breakage, because the smaller eddies have much lower energy (see Eqs. (19)–(20)) and the larger eddies predominantly drag the drop instead of deforming it.

In Ref. [16], the drop breakage time in Eq. (17) is assumed equal to the so-called "deformation time," needed for deforming the drop to a sufficiently large aspect ratio, so that a Rayleigh type of capillary instability could occur. The equation for the deformation time depends on the Reynolds number in the drops, defined as [57]:

$$Re_{DR} = \frac{U_{DIN} d \rho_D}{\eta_D}, \quad (21)$$

where U_{DIN} is the velocity of the liquid inside the drops, and η_D is the dynamic viscosity of the dispersed phase. For our estimates we can use the approximation $U_{DIN} \sim \langle U^2 \rangle^{1/2} \sim (\varepsilon d)^{1/3}$ to obtain:

$$Re_{DR} \sim \frac{d^{4/3} \varepsilon^{1/3} \rho_D}{\eta_D}, \quad (22)$$

which allows us to estimate Re_{DR} from known parameters.

If $Re_{DR} > 1$, which is the typical case for drops with low viscosity, the deformation time is estimated by comparing the

force acting on the drops, due to fluctuations in the dynamic turbulent pressure, to the acceleration of the fluid subdomains in the drop interior, $\nabla P \sim \rho_C \frac{\partial v}{\partial t}$ (see Section 127 in Ref. [57] for detailed explanation). The respective expression for the deformation time reads (cf. with Eq. (127.6) in Ref. [57]):

$$t_{DEF} = \frac{d^{2/3}}{\varepsilon^{1/3}}\sqrt{\frac{\rho_D}{\rho_C}}, \quad Re_{DR} > 1. \tag{23}$$

Combining Eqs. (17)–(23), one derives the following equation for the rate constant of drop breakage:

$$k_{BR} = B_1 \frac{\varepsilon^{1/3}}{d^{2/3}}\sqrt{\frac{\rho_C}{\rho_D}} \exp\left(-B_2 \frac{\sigma}{\rho_D \varepsilon^{2/3} d^{5/3}}\right), \quad Re_{DR} > 1, \tag{24}$$

which is very similar to the original equation proposed in Ref. [16], where the mass densities were not included in the pre-exponential term. B_1 and B_2 are unknown constants, which could be determined from the comparison of the predictions of Eq. (24) with experimental data. From the derivation of Eq. (24) one could expect that the constants B_1 and B_2 are of the order of unity.

In the case of viscous dispersed phase, corresponding to $Re_{DR} < 1$, the drop deformation time should be estimated by neglecting the acceleration term and comparing the pressure fluctuations in the continuous phase with the viscous stress inside the drops (quasi-stationary approximation) [57]. The respective equation reads (cf. with Eq. (127.7) in Ref. [57]):

$$t_{DEF} = \frac{\eta_D}{\varepsilon^{2/3} d^{2/3} \rho_C}, \quad Re_{DR} < 1. \tag{25}$$

Note that t_{DEF} increases with the viscosity of the dispersed phase, η_D, in Eq. (25), whereas it does not depend on η_D in Eq. (23). Furthermore, Eq. (25) predicts that the deformation time decreases with the drop diameter for viscous drops, whereas Eq. (23) for non-viscous drops predicts the opposite trend.

Combining Eqs. (17)–(20) and (25), we obtain the following expression for the breakage rate constant of drops with viscous dispersed phase ($Re_{DR} < 1$), which is a counterpart of Eq. (24):

$$k_{BR} = B_3 \frac{\rho_C d^{2/3} \varepsilon^{2/3}}{\eta_D} \exp\left(-B_4 \frac{\sigma}{\rho_D \varepsilon^{2/3} d^{5/3}}\right), \quad Re_{DR} < 1. \tag{26}$$

Equations (24) and (26) differ in the pre-exponential term, which reflects the different expressions for the deformation times of the less viscous ($Re_{DR} > 1$) and more viscous ($Re_{DR} < 1$) drops. One sees from Eq. (24) that according to this model, the main parameters governing the rate of breakage for $Re_{DR} > 1$ are the average rate of energy dissipation, ε, and the interfacial tension, σ. For viscous drops, $Re_{DR} < 1$, the viscosity of the oil phase, η_D, also affects k_{BR}, see Eq. (26).

The comparison of Eq. (26) with the experimental results (see below) showed that this equation strongly underpredicts the effect of oil viscosity on k_{BR}. For this reason, we modified Eq. (26) to account for the effect of oil viscosity in the activation energy of drop breakage. As shown in our previous study [43], the effect of oil viscosity on the mean and maximum drop diameters for the steady-state drop-size distribution

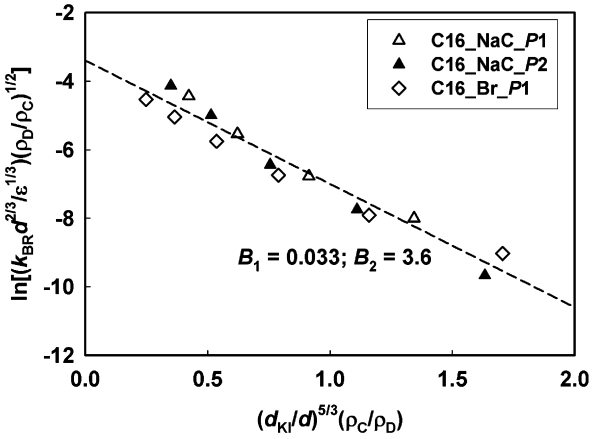

Fig. 6. Comparison of the experimental data for k_{BR}, obtained with hexadecane emulsions, with the model of Coulaloglou and Tavlaridies [16]. The dependence of $\ln[(k_{BR} d^{2/3}/\varepsilon^{1/3})(\rho_D/\rho_C)^{1/2}]$ on $[(d_{KI}/d)^{5/3}(\rho_C/\rho_D)]$ is plotted for emulsions prepared at different values of ε and stabilized by different surfactants. The points are experimental data, whereas the dashed line is the best of the data by Eq. (24). The values of B_1 and B_2 are determined from the fit.

is well described by the Davies' equation [9], which includes a viscosity-related term. Following the same idea, we included an additional exponential term in the expression for k_{BR} to account for the viscous dissipation of energy, E_{DIS}, inside the drops during their breakage:

$$E_{DIS} = \frac{\pi}{6} d^3 \tau_D = \frac{\pi}{6} d^3 \left[\left(\eta_D \varepsilon^{1/3} d^{1/3} \sqrt{\frac{\rho_C}{\rho_D}}\right) \Big/ d\right] = \frac{\pi}{6} \eta_D \varepsilon^{1/3} d^{7/3} \sqrt{\frac{\rho_C}{\rho_D}}. \tag{27}$$

Here τ_D is the viscous stress inside the breaking drop, which is estimated as proposed in Ref. [11]. Thus, the "activation" energy opposing drop deformation is presented as a sum of the surface and dissipated energies, E_σ and E_{DIS}, thus leading to the following equation for k_{BR} (for simplicity, $\rho_D \approx \rho_C$ is assumed):

$$k_{BR}(d) \approx \frac{1}{t_{DEF}} \exp\left[-\frac{(E_\sigma + E_{DIS})}{E_{KIN}}\right] = B_5 \frac{\rho_C d^{2/3} \varepsilon^{2/3}}{\eta_D} \times \exp\left[-B_6 \left(\frac{d_{KI}}{d}\right)^{5/3} \left(1 + B_7 \frac{\eta_D \varepsilon^{1/3} d^{1/3}}{\sigma}\right)\right], \quad Re_{DR} < 1, \tag{28}$$

where B_7 is a constant, which accounts for the relative contribution of the viscous dissipation inside the drops as compared to the surface energy. To the best of our knowledge, Eqs. (26) and (28) for estimate of k_{BR} are original.

To the end of this section we compare our experimental results with the predictions of Eqs. (24), (26) and (28). First, from Eq. (22) we found that $Re_{DR} > 1$ for all hexadecane emulsions studied in the current paper, see Table 1. To compare the experimental data for these emulsions and the corresponding theoretical prediction, we constructed the plot $\ln[(k_{BR} d^{2/3}/\varepsilon^{1/3})(\rho_D/\rho_C)^{1/2}]$ versus $[(d_{KI}/d)^{5/3}(\rho_C/\rho_D)]$,

Table 2
Values of the adjustable constants determined from the best fit to the experimental data by the various theoretical models (see Section 6)

Model equation	Systems		B_σ	B_η
Eq. (24)	Hexadecane	$B_1 = 0.033$	$B_2 = 3.6$	–
Eq. (28)	All, except hexadecane	$B_5 = 0.05$	$B_6 = 11.4$	$B_7 = 0.05$
Eq. (36)	All systems	$B_8 = 0.086$	$B_9 = 5.12$	$B_{10} = A_4 = 0.37$

which should be a "master" straight line, according to Eq. (24); d_{KI} is calculated by Eq. (16). As seen from Fig. 6, the experimental data for the three hexadecane emulsions follow a linear dependence down to drop size $d \approx d_{KI}$, which corresponds to $(d_{KI}/d)^{5/3}(\rho_C/\rho_D) \approx 1.3$. Furthermore, the data for the various hexadecane emulsions fall on the same "master" line, which indicates that Eq. (24) adequately represents the dependence of k_{BR} on d, σ and ε for these emulsions. The adjustable constants found from the best fit to the data are $B_1 = 0.033$ and $B_2 = 3.6$ (see Table 2); these values are discussed in Section 6.4.

For the emulsions of more viscous oils (SBO and silicone oils), the estimated values of Re_{DR} become smaller than unity for drops with given diameter, d_{RE}, which depends on the specific system, see Eq. (22) and Table 1. Note also that according to Eq. (24), k_{BR} should not depend on the oil viscosity, which contradicts the experimental results (see Fig. S1). Therefore, for drops with $d < d_{RE}$ we should use Eq. (26) or (28), instead of Eq. (24). In accordance with Eq. (26), we constructed the plot $\ln[k_{BR}\eta_D/(\rho_C d^{2/3}\varepsilon^{2/3})]$ versus $[(d_{KI}/d)^{5/3}(\rho_C/\rho_D)]$, which should correspond to a "master" straight line. As seen from Fig. 7a, the experimental points do not fall on a straight line or on a single "master" curve—the data for oils with various viscosities differ very significantly from each other. Therefore, the observed effect of oil viscosity on k_{BR} cannot be described by Eq. (24) or (26).

In contrast, the comparison of the experimental data with the predictions of Eq. (28), shown in Fig. 7b, revealed much better agreement between experiment and theory. One sees that the experimental data fall on almost linear dependence and converge to a single "master" line, when the appropriate plot corresponding to Eq. (28) is used. The values of the adjustable constants $B_5 = 0.05$, $B_6 = 11.4$, and $B_7 = 0.05$ were determined from the best fit to the data and are all rather reasonable (see Section 6.4 for discussion). It is worthwhile noting that the results for hexadecane emulsions with $Re_{DR} > 1$ (not shown in Fig. 7), did not comply with Eq. (28), which emphasizes the need for using appropriate expressions for the deformation times of less viscous and more viscous drops [57].

We can conclude that the experimental data for $k_{BR}(d)$ for hexadecane emulsions are reasonably well described by the model proposed in Ref. [16]. However, this model is inapplicable to emulsions prepared with more viscous oils (such as SBO and silicone oils), for which $Re_{DR} < 1$. We described these emulsions after modifying the model from Ref. [16] by: (1) using appropriate equation for the deformation time of viscous drops, and (2) accounting for the effect of energy of viscous dissipation inside the breaking drops—see Eq. (28).

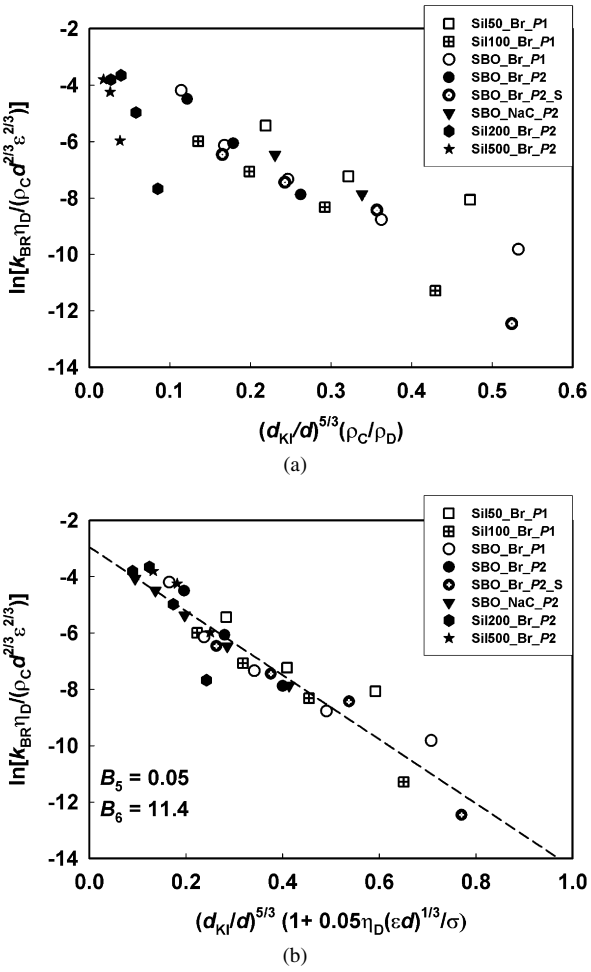

Fig. 7. Comparison of the experimental data for k_{BR} with the model based on drop deformation time, for drops with $Re_{DR} < 1$ (viscous oils). The points are experimental data for different systems, whereas the line in (b) is the best fit according to Eq. (28). The data do not merge into a single master line on (a), which shows that Eq. (26) does not describe well the systems studied.

6.2. Models based on the drop–eddy collision frequency

In the model proposed by Prince and Blanch [18] and by Tsouris and Tavlaridies [19], the breakage rate is assumed to be proportional to the frequency of drop–eddy collisions and the breakage efficiency:

$$v_{BR} = (\text{eddy–drop collision frequency}) \times (\text{breakage efficiency}). \quad (29)$$

The probability for drop–eddy collisions is estimated by analogy with the molecular collision theory of gases. The collision frequency $h(d)$ between drops of size d and eddies of size d_e that can break these drops (i.e., eddies with size equal or smaller than drop diameter) is presented as [18]:

$$h(d) = \int_{n_e} S_{d,e}\left(U_d^2 + U_e^2\right)^{1/2} n_d \, dn_e, \quad (30)$$

where $S_{d,e} = \frac{\pi}{4}(d_e + d)^2$ is the collision cross-section area; n_d is the number concentration of drops with size d; U_d is the mean drop velocity; dn_e is the number concentration of eddies

with size between d_e and $d_e + \delta d_e$; and U_e is the mean velocity of these eddies. The number concentration of the eddies can be determined from the expression [18,58]:

$$\mathrm{d}n_e(\kappa) \approx \frac{0.1\kappa^2}{\rho_C}\,\mathrm{d}k. \tag{31}$$

Here $n_e(\kappa)$ is the number concentration of eddies with wave number $\kappa \approx 2/d_e$ per unit mass of the fluid, and ρ_C is the mass density of the continuous phase.

In this approach [18,19], the efficiency of drop breakage is expressed by the equation:

$$Y(d) = \exp\left(-\frac{E_\sigma}{E_{KIN}}\right), \tag{32}$$

where E_σ is the drop surface energy given by Eq. (18), whereas E_{KIN} is the kinetic energy of the eddies, expressed as [19]:

$$E_{KIN} = 0.43\pi\rho_C(2/\kappa)^{11/3}\varepsilon^{2/3}. \tag{33}$$

Thus, the final equation for the breakage rate constant in this model reads [19]:

$$k_{BR}(d) = 0.1\frac{\pi}{4}\varepsilon^{1/3}\int_{2/d}^{2/\lambda_0}\left(\frac{2}{\kappa}+d\right)^2\left(8.2\kappa^{-2/3}+1.07d^{2/3}\right)^{1/2} \times \kappa^2\exp\left(-\frac{E_\sigma}{E_{KIN}}\right)\mathrm{d}\kappa, \tag{34}$$

where λ_0 is the size of the smallest eddies in the system.

If one assumes that most efficient for drop breakage are the collisions of the drops with eddies of similar size (because these eddies have highest kinetic energy from all eddies able to deform the drops [57,59]), one derives the following expression for the rate constant of drop breakage, which is a simplified version of Eq. (34):

$$k_{BR}(d) \sim \frac{\varepsilon^{1/3}}{d^{2/3}}\exp\left(-\frac{\sigma}{\rho_C\varepsilon^{2/3}d^{5/3}}\right). \tag{35}$$

The pre-exponential term in the above equation arises from the frequency of eddy–drop collisions, whereas the exponential term accounts for the breakage efficiency. It is seen that Eq. (35) is very similar in structure to Eq. (24), with the only difference that the density of the continuous phase, instead of that of the dispersed phase, appears in the exponential term (see the discussion on this point in Ref. [18]). Since $\rho_C \approx \rho_D$ in most emulsions, Eqs. (24) and (35) predict very similar numerical results. It is obvious that we cannot describe the experimentally observed dependence of k_{BR} on the oil viscosity by Eq. (35), because η_D does not appear in this equation. Therefore, following the same argumentation as in Section 6.1, we included in the exponent of Eq. (35) a term, accounting for the viscous dissipation inside the drops:

$$k_{BR}(d) = B_8\frac{\varepsilon^{1/3}}{d^{2/3}}\exp\left[-B_9\left(\frac{d_{KI}}{d}\right)^{5/3}\left(1+B_{10}\frac{\eta_D\varepsilon^{1/3}d^{1/3}}{\sigma}\right)\right], \tag{36}$$

where B_8, B_9, and B_{10} are unknown constants.

According to Eq. (36), the experimental data for the various systems should fall on a master line, if the following scaling is used:

$$\ln\left(\frac{k_{BR}(d)d^{2/3}}{\varepsilon^{1/3}}\right) = \ln(B_8) - B_9\left(\frac{d_{KI}}{d}\right)^{5/3}\left(1+B_{10}\frac{\eta_D(\varepsilon d)^{1/3}}{\sigma}\right), \tag{37}$$

where d_{KI} is defined by Eq. (16); B_8, B_9, and B_{10} appear as adjustable constants (which could be found by best fit to the experimental data); and all remaining parameters are known. Since B_{10} accounts for the relative contribution of the viscous dissipation in the breaking drop (as compared to the contribution of the capillary pressure) one should expect this constant to be the same as the one appearing in Eq. (15) for the maximum stable drop diameter, d_{MAX}. Therefore, in the following consideration we fixed the value $B_{10} = A_4 = 0.37$, whereas the values of B_8 and B_9 were determined from the best fit to the data. Note that this assumption allows us to describe both d_{MAX} at steady state and the kinetic constants k_{BR} (leading to this steady state) by a self-consistent approach.

As seen from Fig. 8, the experimental data for all systems (except for the silicone oil with viscosity 500 mPa s—see below for explanation on this point) indeed fall on a linear dependence down to drop diameter $d \approx d_{KI}$ (the last points on the right-hand side). This plot indicates that Eq. (36) adequately represents the dependence of k_{BR} on the drop diameter, oil viscosity (up to 200 mPa s), interfacial tension, and rate of energy dissipation for all systems studied. The obtained values of $B_8 = 0.086$ and $B_9 = 5.12$ are reasonable and are discussed in Section 6.4 below. Note that Eq. (36) has the advantage over Eqs. (24), (26)

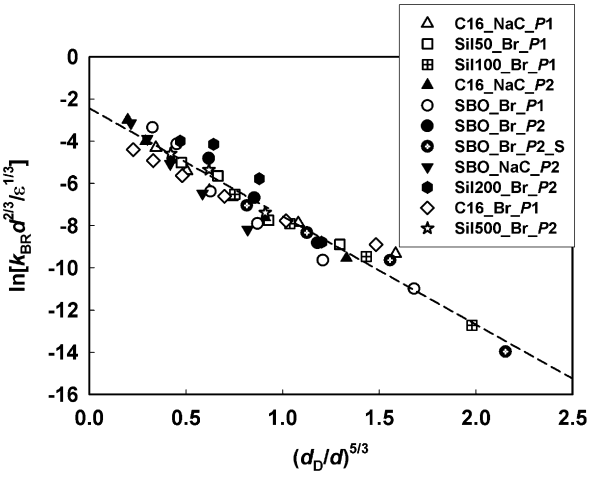

Fig. 8. Comparison of the experimental data for k_{BR} for all emulsions studied (the symbols) with the predictions of Eq. (37) (the dashed line). The logarithm of the normalized breakage rate constants, $\ln(k_{BR}d^{2/3}/\varepsilon^{1/3})$, is plotted as a function of the inverse normalized diameter of the drops, d_D/d. The Davies diameter, d_D, is calculated from Eq. (15), except for the silicone oil with $\eta_D = 494$ mPa s, for which the experimental value of the maximum diameter was used, $d_D = d_{V95}$. The adjustable constants $B_8 = 0.086$ and $B_9 = 5.12$ are determined from the best fit to the data. The constant accounting for the relative effect of oil viscosity on drop breakage, $B_{10} = A_4 = 0.37$, was taken to be the same as that for the maximum drop diameter [43].

and (28) in being able to describe all systems studied, including those of less viscous and more viscous oils.

It is worthwhile noting that Eq. (37) with $B_{10} = A_4 = 0.37$ (taken to be the same as in Eq. (15) for d_D), could be represented in the form:

$$\ln\left(\frac{k_{BR}(d)d^{2/3}}{\varepsilon^{1/3}}\right) = \ln(B_8) - B'_9\left(\frac{d_D}{d}\right)^{5/3}, \tag{37a}$$

where d_D is defined by Eq. (15) and $B'_9 = B_9/A_3 = 5.94$. The combination of Eqs. (15) and (37a) is very convenient for estimates of k_{BR}. For example, we can easily estimate that in our systems $k_{BR} < 0.2\ s^{-1}$ (i.e., $k_{BR} \approx 0$ in the timeframe and accuracy of our experiments) for drops with $d \leqslant d_K \approx 0.7d_D$, because the argument of the logarithm in the left-hand side of Eq. (37a) is $\approx 2 \times 10^{-6}$ and $\varepsilon^{1/3}/d^{2/3} \sim 10^5$.

We found that the experimental data for the most viscous silicone oil with $\eta_D \approx 500$ mPa s deviate from the master curve in Fig. 8, if the plot corresponding to Eq. (37) is used. The latter observation is related to the fact that the value of d_D calculated by Eq. (15) is higher than the experimentally determined value for this oil—see the discussion of Fig. 6 in Ref. [43]. That is why, we used the experimental value of d_{V95} (instead of d_D) to plot the data in Fig. 8 for this oil, and found a reasonably good description by Eq. (37a)—see the "stars" in Fig. 8, which fall very close to the theoretical dashed line.

In conclusion, Eq. (36), based on the drop–eddy collision frequency is able to describe relatively well the experimental data for k_{BR} for all systems studied with the values $B_8 = 0.086$, $B_9 = 5.12$, and $B_{10} = 0.37$.

6.3. Other models

In Ref. [55], the drop–eddy collisions are described as a Poisson process, and k_{BR} is evaluated by the equation:

$$k_{BR} = B_{11}\varepsilon^{1/3} \times \operatorname{erfc}\left(\sqrt{B_{12}\frac{\sigma}{\rho_C\varepsilon^{2/3}d^{5/3}} + B_{13}\frac{\eta_D}{\sqrt{\rho_C\rho_D}\varepsilon^{1/3}d^{4/3}}}\right), \tag{38}$$

where B_{11} is an empirical constant with dimensions $m^{-2/3}$, and B_{12} and B_{13} are dimensionless constants. The meaning of B_{13} is similar to that of our constant A_4 in Eqs. (15) and (37)—it accounts for the relative contribution of the viscous dissipation inside the breaking drops. Assuming $B_{13} = A_4 \approx 0.37$, we obtain the following simplified form of Eq. (38):

$$k_{BR} = B_{11}\varepsilon^{1/3}\operatorname{erfc}\left(\sqrt{B'_{12}\left(\frac{d_D}{d}\right)^{5/3}}\right). \tag{38a}$$

To check the applicability of the above equation to our data, we plot in Fig. S4 the function $k_{BR}/\varepsilon^{1/3}$ versus $(d_D/d)^{5/6}$ for all emulsions studied. As seen from Fig. S4, the data from the various systems do not merge toward a single master curve, which means that Eq. (38a) does not describe our data with a unique pair of values of B_{11} and B'_{12}.

In the so-called "kinematic" type of models, k_{BR} is assumed equal to the inverse drop breakage time, which is determined from the stress balance including the drop capillary pressure and the viscous stress inside the breaking drop [22,23]. The period, during which the stress of the continuous phase acts on the drop surface, is assumed equal to the eddy lifetime. The expression proposed for k_{BR} in Refs. [22,23] contains a function describing the breakage probability of the larger drop into two smaller drops of unequal sizes. However, we found experimentally that the breakage of a large drop in our systems leads to formation of multiple small drops [35]. Therefore, the assumption for binary drop breakage, used in Ref. [22,23] to derive the expression for k_{BR}, is not applicable to our systems. For this reason, we have not attempted to describe our data by the expressions from Refs. [22,23] or their modifications. Another model for k_{BR} was proposed in Ref. [24], however, it does not account for the effect of oil viscosity and, therefore, it could not describe all of our results.

6.4. Discussion—comparison of the various models

The comparison of the various models with the experimental data, discussed in Sections 6.1–6.3, shows that we can describe adequately the experimental data for k_{BR} by Eq. (24) for hexadecane emulsions in which the Reynolds number $Re > 1$, and by Eq. (28) for the other systems, in which $Re < 1$, see Figs. 6 and 7b. On the other hand, the experimental data for all systems could be described by Eq. (36), as well (see Fig. 8). The other models tested do not describe adequately the experimental data. The values of the adjustable constants appearing in Eqs. (24), (28), and (36) found from the best fit of the experimental data are all reasonable (see Table 2).

The comparison of the models with the experimental data shows also that the values of k_{BR} for the viscous oils could be adequately described only when the term accounting for the viscous dissipation inside the breaking drops is included in the energy balance for the breakage efficiency (i.e., in the exponential terms in Eqs. (28) and (36)). The fact that Eq. (24) describes relatively well the experimental data for hexadecane (despite the absence of such viscous term), is explained by the negligible contribution of the viscous term in comparison with the term accounting for the surface energy of the deforming drop. Therefore, the most important conclusion from the screening of the theoretical expressions is that for all systems studied and for both types of models described in Sections 6.1 and 6.2, the breakage efficiency, $Y(d)$, is well represented by the relation:

$$Y(d) \sim \exp\left(-\frac{E_\sigma + E_{DIS}}{E_{KIN}}\right) \sim \exp\left(-B_\sigma\frac{E_\sigma}{E_{KIN}}\left(1 + B_\eta\frac{E_{DIS}}{E_\sigma}\right)\right), \tag{39}$$

where E_σ is the surface energy, E_{DIS} is the energy dissipated inside the drop, and E_{KIN} is the mean kinetic energy of the turbulent eddies of size d. The numerical constants B_σ and B_η account for the drop surface deformation and for the viscous dissipation inside the breaking drops, respectively. The specific values of B_σ and B_η, however, depend on the chosen type of the pre-exponential term (drop deformation time or drop–eddy collision frequency), see Table 2.

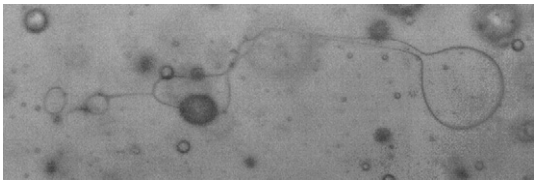

Fig. 9. Image of a breaking drop of silicone oil with $\eta_D = 500$ mPa s, stabilized by 1 wt% Brij 58. The image is taken by a high-speed video camera (model PCO.1200hs, Samwoo Scientific Co., 700 frames/s) in a homogenizer equipped with optical window, which allows optical observation of the drops just after the narrow slit of the processing element.

It is worthy to emphasize two specific advantages of the model based on the drop–eddy collision frequency, Eq. (36): (1) The experimental results for all systems are described by a single equation; and (2) The constant B_η entering this model has the same meaning and value as the constant $A_\eta = A_4$ appearing in Eq. (15) to describe the maximum drop size in the emulsions, i.e., the kinetics of drop breakage and the maximum diameter of the stable drops are described by a self-consistent approach.

Let us note at the end of this discussion that, although Eq. (36) describes all main characteristics of the studied emulsions (see also Figs. 6, 7 and S1 in Ref. [35]), its terms have clear physical meaning, and all adjustable constants have the right order of magnitude, one cannot prove unambiguously that this is the only model relevant to these systems. For example, as explained above, the same set of experimental data could be described by a combination of two equations for oils with high and low viscosities, respectively. Another deficiency of the model originates from the discretization scheme used to determine k_{BR} (Section 3). Due to the discrete size-domains in the kinetic scheme, the model neglects the possibility for formation of very big daughter drops, which would fall in the same size-domain as the breaking drop. Such a possibility (which would lead to underestimated values of k_{BR} in our analysis) could not be ruled out and could affect seriously the results, if the drop breakage was of "erosive type," that is, if the daughter drops were formed predominantly through "biting" small fractions of the breaking drop by colliding turbulent eddies. However, as explained in Ref. [35], our experimental results indicate that the predominant mode of daughter drop formation is capillary instability of long oil threads, formed after a strong deformation of the breaking drop—see Fig. 9, where an illustrative image of a breaking drop is shown. This mode of drop breakage strongly reduces the probability for formation of very big daughter drops that would fall in the same size-domain as the breaking drop. Therefore we do not expect that our final results, and Eq. (36) in particular, are strongly affected by the used discretization scheme of data interpretation.

7. Comparison of our results with experimental data by other authors

In this section we briefly compare our results for k_{BR} with two sets of experimental results reported by other authors [32,38].

The effects of several factors (hydrodynamic conditions, interfacial tension and oil viscosity) on k_{BR}, for emulsions prepared in stirred tanks, were studied by Sathyagal et al. [38]. The experimental results were fitted by an empirical equation, which accounted for the effects of all these factors (Eq. (5) in [38]). When we tried to describe our experimental results by this equation (using the numerical constants from Ref. [38]), we calculated significantly lower values of k_{BR} than those found experimentally in the current study. Our analysis showed that this discrepancy could be related to two main reasons: (1) To find the dependence of k_{BR} on the hydrodynamic conditions during emulsification, the authors of Ref. [38] used the mean value of ε in the stirred tank. As discussed in Ref. [43], this definition of ε leads to rather different values of the estimated maximum drop size, d_D, as compared to our experimental data for d_{V95}. One could expect that similar problem with the definition of ε appears when trying to describe the data for k_{BR}. (2) The emulsification time, $\theta = t_{EM}$, is defined in Ref. [38] to be equal to the residence time of the drops in the entire stirred tank, including the zones where the rate of energy dissipation is relatively low. In contrast, in our study θ is defined as the time, during which the drops actually reside in the most active zone of the homogenizer, where the rate of energy dissipation is highest. For both types of homogenizer (narrow gap and stirred tanks), the volume of the most active zones, V_{DIS}, is much smaller than the total volume of the homogenizer, which means that the actual residence time in the active zone is much shorter than the total emulsification time, $\theta \ll t_{EM}$. Therefore, conceptually different definitions of θ are used in Ref. [38] and in our study. Our preliminary numerical checks showed that these different definitions of θ lead to significant difference in the calculated values of k_{BR} from the same set of experimental data ($k_{BR} \propto 1/\theta$, where θ is the assumed residence time). In conclusion, to compare properly the predictions of Eq. (5) from Ref. [38] with our results, we should rescale both the residence time and the rate of energy dissipation. Although this task could be potentially useful, it is by no means trivial and falls beyond the scope of the current study.

In Ref. [32] the probability for drop breakage of single oil drops passing through a narrow constriction, was determined by optical observations. The results for the drop breakage probability were represented by the following expression (Eq. (12) in Ref. [32]):

$$P_{BR}(d) = a_1 \exp\left(-a_2 \frac{\sigma}{2\rho_C \varepsilon^{2/3} d^{5/3}}\right). \tag{40}$$

From the best fit to the data, the values $a_1 = 2.6$ and $a_2 = 11.2$ were determined [32]. The experiments were performed with n-heptane having a viscosity of 0.45 mPa s, hence, the viscous dissipation inside the drops is expected to be negligible. Therefore, the results from Ref. [32] should be compared to our results with hexadecane-in-water emulsions. From the comparison of Eqs. (36) and (40) one sees that B_9 should be equal to $a_2/2$ to have an agreement between our results and those in Ref. [32]. Indeed, we found $B_9 = 5.1$ in our experiments, which is very close to the value of $a_2/2 = 5.6$ found in [32]. Thus we can conclude that we have rather reasonable agreement between

our results and those of Ref. [32] (the value a_1 in Eq. (40) cannot be directly compared to any of the constants determined in our study).

8. Conclusions

Systematic set of experiments is performed to monitor the evolution of the drop-size distribution, as a function of the emulsification time, in turbulent flow generated in a narrow-gap homogenizer. The effects of the viscosity of the oil phase, η_D, interfacial tension, σ, and rate of energy dissipation in the turbulent flow, ε, are studied. The experimental data are interpreted by using a kinetic scheme, which allows us to determine the rate constant of drop breakage, k_{BR}, as a function of drop diameter, d, and the other factors studied.

The experimental results show that k_{BR} rapidly decrease with the decrease of drop diameter and the breakage process becomes negligible, when d becomes smaller than the Davies' diameter, d_D, as estimated from Eq. (15). Also, k_{BR} rapidly decreases with the increase of η_D and σ, and with the decrease of ε. The relation between the experimentally determined maximum drop diameter, the kinetics of drop breakage, and the total emulsification time is discussed.

The experimental results for k_{BR} are compared with theoretical models, proposed in the literature, and with their modifications. Following the approach by Prince and Blanch [18] we proposed a new theoretical expression, which considers k_{BR} as a product of the collision frequency between drops and eddies with similar size, multiplied by a factor, accounting for the breakage efficiency. The breakage efficiency includes the contributions of the surface extension energy and the energy dissipated inside the breaking drop. The proposed expression for k_{BR}, Eq. (36), describes reasonably well the experimental data for all systems studied. Two important advantages of this expression are that: (1) it describes data for both oils with low and high viscosity (up to 500 mPa s), and (2) it is consistent with the expression describing the maximum diameters of the stable drops in the formed emulsions, Eq. (15), viz. the constants expressing the relative contribution of the energy dissipated inside the breaking drop are equal, $A_4 = B_{10}$.

Acknowledgments

The authors are grateful to Prof. I.B. Ivanov for the numerous and very useful discussions, and for the critical reading of the manuscript. The useful discussion with Prof. M. Kostoglou (Aristotle Univ. Thessaloniki, Greece) is gratefully acknowledged. The valuable experimental help by D. Sidzhakova and the help in drop-size determination by M. Paraskova and E. Kostova (all from the Sofia University) are deeply appreciated. This study was supported by BASF Aktiengesellschaft, Ludwigshafen, Germany.

Appendix A. Notation

To save space, only the notation that did not appear in the first paper of this series, Ref. [43], is listed below.

A.1. Capital latin letters

B	numerical constants in equations for k_{BR}
B_1, B_2	Eq. (24)
B_3, B_4	Eq. (26)
B_5, B_6, B_7	Eq. (28)
B_8, B_9, B_{10}	Eq. (36)
B'_9	Eq. (37a)
B_{11}, B_{12}, B_{13}	Eq. (38)
B'_{12}	Eq. (38a)
B_σ, B_η	numerical constants accounting, respectively, for the effects of the capillary pressure and of the viscous dissipation inside the breaking drop
E	energy
E_{DIS}	energy dissipated inside the breaking drop due to viscous stresses
E_{KIN}	mean kinetic energy of the turbulent eddies of size d
E_σ	drop surface energy
N_S	number of drops in the interval with average diameter d_S
$P_{BR}(d)$	probability for drop breakage, Eq. (40)
Re_{DR}	Reynolds number of the liquid inside the drops
$S_{d,e}$	cross-section area of drop–eddy collisions, defined as $S_{d,e} = \pi(d + d_e)^2/4$
U	velocity
U_{DIN}	velocity of the liquid inside the drops
U_d	mean drop velocity
U_e	mean velocity of turbulent eddies with size
V	volume
V_{EM}	total emulsion volume
V_{OIL}	total volume of emulsified oil
We	Weber number, defined as $\mathrm{We} = Pd/\sigma$
$Y(d)$	efficiency of drop breakage

A.2. Small latin letters

a_1, a_2	dimensionless numerical constants, Eq. (40)
d	drop diameter
$d_0, d_1, d_2, \ldots, d_S, d_{S+1}, d_{S+2}, \ldots, d_{N-3}, d_{N-2}, d_{N-1}, d_N$	average diameters of the intervals, in which the drops are classified; d_0 is the smallest drop diameter; d_N is the largest drop diameter; d_S is defined as $d_S = \sqrt[3]{2^S} d_0$; S is an integer between 0 and N
d_K	diameter of the largest drops, which could not break
d_M	diameter of a "mother" drop, which breaks into "daughter" drops with diameters in the range between d_0 and d_{M-1} ($K < M \leqslant N$)
d_{MAX}	maximum diameter of the stable drop
d_{RE}	diameter of drops with $Re_{DR} = 1$
d_{32}^{INI}	mean volume-surface diameter of the initial oil–water premix, prepared by membrane emulsification
$h(d)$	frequency of collisions between drops of diameter d and eddies of size d_e
k	rate constant of drop breakage
$k_{BR}, k_{BR}(d)$	breakage rate constant
k_M	breakage rate constant for drops with diameter d_M
$k_S, k_S(d_S)$	breakage rate constant for drops with diameter d_S

k_N breakage rate constant for the largest drops (with diameter d_N)

k_{N-1}, k_{N-2} breakage rate constants for drops with diameters d_{N-1} and d_{N-2}

n number concentration

n_d number concentration of drops with diameter d

$n_e(\kappa)$ number concentration of turbulent eddies with wave number κ

dn_e number concentration of turbulent eddies with size between d_e and $d_e + \delta d_e$

$n_M(x)$ number concentrations of mother (breaking) drops with diameter d_M, along the processing element

$n_N(x)$ number concentration of the largest drops with diameter d_N along the processing element

$n_S \equiv n(d_S)$ number concentration of drops with average diameter d_S

$n_S(x,u), n_S(x)$ number concentration of drops with average diameter, d_S, as a function of the distance from the entrance of the processing element, x, and of the number of emulsion passes through the homogenizer, u

$n_N^0, n_{N-1}^0, \ldots, n_S^0$ number concentrations of drops with diameters d_N, d_{N-1}, and d_S in the initial emulsion, prepared by membrane emulsification

p probability for daughter drop formation

$p_{S,M}$, $p_{S,M}(d_S, d_M)$ average volume fraction of a mother drop with diameter d_M, which is transformed into daughter drops with diameter d_S $(0 \leqslant S \leqslant M-1;\ S < M \leqslant N)$

$(2^{M-S} p_{S,M})$ average number of drops with diameter d_S, formed after breakage of a mother drop with diameter d_M

t time

t_{EM} total time of emulsification; in our experiments equal to $u\theta$

t_{EXP} characteristic time of the experiment ($t_{EXP} = 100\theta$ in our experiments)

t_{BR} drop breakage time

t_{DEF} drop deformation time

u number of passes of the emulsion through the homogenizer

v_{BR} rate of drop breakage

v volume

$v_0, \ldots, v_S, v_{S+1}, \ldots, v_N$ average volumes of the drops falling in the respective intervals with diameters $d_0, \ldots, d_S, d_{S+1}, \ldots, d_N$

v_0 volume of the smallest drops with diameter d_0

v_M volume of a mother drop with diameter d_M

x distance from the beginning of the processing element, Fig. 2

y_S lower boundary of the interval with average diameter d_S

$\Delta y_S = (y_{S+1} - y_S)$ width of the interval with average diameter d_S

A.3. Small greek letters

κ wave number of the turbulent eddies, defined as $\kappa \sim 2/d_e$

ν average total number of daughter drops, formed after breakage of a mother drop

θ residence time of the drops in the processing element, defined as $\theta = (L/U_1)$

τ_D viscous stress inside the breaking drop

A.4. Abbreviations

PBE population balance equation.

SPG1.1, SPG3.2, SPG10.7, SPG19.3 Shirasu Porous Glass membranes with different mean pore size in micrometers.

Supporting materials

The online version of this article contains additional supplementary material.

Please visit DOI: 10.1016/j.jcis.2007.04.064.

References

[1] A.N. Kolmogorov, C. R. Acad. Sci. URSS 66 (1949) 825.
[2] J.O. Hinze, AIChE J. 1 (1955) 289.
[3] F.B. Sprow, Chem. Eng. Sci. 22 (1967) 435.
[4] H.T. Chen, S. Middleman, AIChE J. 13 (1967) 989.
[5] C.A. Sleicher, AIChE J. 8 (1962) 471.
[6] J. Baldyga, W. Podgorska, Can. J. Chem. Eng. 76 (1998) 456.
[7] J.F. Walter, H.W. Blanch, Chem. Eng. J. 32 (1986) B7.
[8] S.M. Bhavaraju, T.W.F. Russel, H.W. Blanch, AIChE J. 24 (1978) 454.
[9] J.T. Davies, Chem. Eng. Sci. 40 (1985) 839.
[10] J.S. Lagisetty, P.K. Das, R. Kumar, K.S. Gandhi, Chem. Eng. Sci. 41 (1986) 65.
[11] R.V. Calabrese, T.P.K. Chang, P.T. Dang, AIChE J. 32 (1986) 657.
[12] C.Y. Wang, R.V. Calabrese, AIChE J. 32 (1986) 667.
[13] R.V. Calabrese, C.Y. Wang, N.P. Bryner, AIChE J. 32 (1986) 677.
[14] P.D. Berkman, R.V. Calabrese, AIChE J. 34 (1988) 602.
[15] J.C. Lasheras, C. Eastwood, C. Martinez-Bazan, J.L. Montanes, Int. J. Multiphase Flow 28 (2002) 247.
[16] C.A. Coulaloglou, L.L. Tavlarides, Chem. Eng. Sci. 32 (1977) 1289.
[17] M. Konno, Y. Matsunaga, K. Arai, S. Saito, J. Chem. Eng. Jpn. 16 (1980) 67.
[18] M.J. Prince, H.W. Blanch, AIChE J. 36 (1990) 1485.
[19] C. Tsouris, L.L. Tavlarides, AIChE J. 40 (1994) 395.
[20] H. Luo, F. Svendsen, AIChE J. 42 (1996) 1225.
[21] D.K.R. Nambiar, R. Kumar, T.R. Das, K.S. Gandhi, Chem. Eng. Sci. 47 (1992) 2989.
[22] D.K.R. Nambiar, R. Kumar, T.R. Das, K.S. Gandhi, Chem. Eng. Sci. 49 (1994) 2194.
[23] C. Martinez-Bazan, J.L. Montanes, J.C. Lasheras, J. Fluid Mech. 401 (1999) 157.
[24] C. Eastwood, A. Cartellier, J.C. Lasheras, in: Advances in Turbulence VIII, Proceedings of 8 European Turbulence Conference, Barselona, 2000, p. 273.
[25] M. Kostoglou, S. Dovas, A.J. Karabelas, Chem. Eng. Sci. 52 (1997) 1285.
[26] M. Kostoglou, A.J. Karabelas, Chem. Eng. Sci. 53 (1998) 505.
[27] M. Kostoglou, A.J. Karabelas, J. Phys. A Math. Gen. 31 (1998) 8905.
[28] M. Kostoglou, A.J. Karabelas, Chem. Eng. Sci. 56 (2001) 4283.
[29] M. Kostoglou, A.J. Karabelas, Chem. Eng. Sci. 60 (2005) 6584.
[30] M. Kostoglou, A.J. Karabelas, J. Colloid Interface Sci. 284 (2005) 571.
[31] M. Konno, M. Aoki, S. Saito, J. Chem. Eng. Jpn. 16 (1983) 312.
[32] S. Galinat, O. Masbernat, P. Guiraud, C. Dalmazzone, C. Noik, Chem. Eng. Sci. 60 (2005) 6511.
[33] H. Sis, S. Chander, Colloids Surf. A 235 (2004) 113.
[34] H. Sis, G. Kelbaliyev, S. Chander, J. Dispersion Sci. Technol. 26 (2005) 565.

[35] S. Tcholakova, N. Vankova, N.D. Denkov, T. Danner, J. Colloid Interface Sci. 310 (2007) 570.
[36] G. Narsimhan, D. Ramkrishna, J.P. Gupta, AIChE J. 26 (1980) 991.
[37] G. Narsimhan, G. Nejfelt, D. Ramkrishna, AIChE J. 30 (1984) 457.
[38] A.N. Sathyagal, D. Ramkrishna, G. Narsimhan, Chem. Eng. Sci. 9 (1996) 1377.
[39] A.N. Sathyagal, D. Ramkrishna, G. Narsimhan, Comput. Chem. Eng. 19 (1995) 437.
[40] S. Tcholakova, N.D. Denkov, D. Sidzhakova, I.B. Ivanov, B. Campbell, Langmuir 19 (2003) 5640.
[41] S. Tcholakova, N.D. Denkov, T. Danner, Langmuir 20 (2004) 7444.
[42] H. Steiner, R. Teppner, G. Brenn, N. Vankova, S. Tcholakova, N.D. Denkov, Chem. Eng. Sci. 61 (2006) 5841.
[43] N. Vankova, S. Tcholakova, N.D. Denkov, I.B. Ivanov, V. Vulchev, T. Danner, J. Colloid Interface Sci., doi: 10.1016/j.jcis.2007.03.059.
[44] A.G. Gaonkar, R.P. Borwankar, Colloids Surf. 59 (1991) 331.
[45] K. Kandori, in: A.G. Gaonkar (Ed.), Food Processing: Recent Developments, Elsevier, Amsterdam, 1995, pp. 113–142.
[46] K. Kandori, K. Kishi, T. Ishikawa, Colloids Surf. 62 (1991) 269.
[47] H. Yoshizawa, H. Ohta, Y. Hatate, J. Chem. Eng. Jpn. 29 (1996) 1027.
[48] N. Christov, D.N. Ganchev, N.D. Vassileva, N.D. Denkov, K.D. Danov, P.A. Kralchevsky, Colloids Surf. A 209 (2002) 83.
[49] T. Nakashima, M. Shimizu, Chem. Eng. Symp. Ser. 21 (1988) 93.
[50] R. Bleck, J. Geophys. Res. 75 (1970) 5165.
[51] S. Kumar, D. Ramkrishna, Chem. Eng. Sci. 51 (1996) 1311.
[52] C. Hill, An Introduction of Chemical Engineering Kinetics & Reactor Design, Wiley, New York, 1977, chap. 8.
[53] C. Orr, in: Encyclopedia of Emulsion Technology, Dekker, New York, 1983, chap. 6.
[54] G. Narsimhan, J.P. Gupta, D. Ramkrishna, Chem. Eng. Sci. 34 (1979) 257.
[55] V. Alopaeus, J. Koskinen, K. Keskinen, J. Majander, Chem. Eng. Sci. 57 (2002) 1815.
[56] G.K. Batchelor, An Introduction to Fluid Dynamics, Cambridge Univ. Press, Cambridge, 1967.
[57] V.G. Levich, Physicochemical Hydrodynamics, Prentice–Hall, Englewood Cliffs, NJ, 1962.
[58] D. Azbel, I.L. Athanasios, in: N. Cheremisinoff (Ed.), Handbook of Fluids in Motion, Ann Arbor Science Publisher, Ann Arbor, MI, 1983, p. 473.
[59] B. Shreekumar, R. Kumar, K.S. Gandhi, J. Fluid Mech. 328 (1996) 1.